SUDAN UNIVERSITY OF SCIENCE AND TECHNOLOGY
COLLEGE OF GRADUATE STUDIES

USE OF FINITETIME THERMODYNAMIC SIMULATION OF PERFORMANCE OF AN OTTO CYCLE WITH VARIABLE SPECIFIC HEATS OF WORKING FLUID

استخدام الحركيات الحرارية محدودة الزمن لمحاكاة اداء دورة أوتو ذات سعات حرارية متغيرة لمائع التشغيل

A Thesis Submitted in Partial Fulfillment of the Degree of M.Sc. IN MECHANICAL ENGINEERING (Power)

Prepared by:

Jalaa Azhari Abd Alla Abd AlMajeed

Supervisor:

Dr. Ali Mohammed Hamdan Adam

October 2018

Dedication

I dedicated this message to my dear father, mother and sisters, my beloved husband, "Ahmed Dafalla" and our sweet daughter Layan.

I also dedicate this work to my colleagues and everyone who contributed with me and stood by me.

Acknowledgement

First of all, giving thanks to Allah,
And a special thanks to my supervisor

DR. ALI MOHAMMED HAMDAN ADAM.

I can't forget giving thanks to everyone who helped me and gave me a new hope for successful.

I am gratefully acknowledges the lectures and all the staff of Sudan University's, Department of Mechanical Engineering for all what they offered throughout my educational path in the university.

At the last "thanks" for every one stood beside me until the last dot.

Abstract

A finitetime thermodynamic modelling and simulation of irreversible Otto cycle engines has been developed taking into account the variability of specific heats for working fluid due to temperature variation. The effect of three different parameters on the engine was discussed, which are: the internal irreversibility, the heat losses and the friction losses. A program was developed by using MATLAB software to perform the necessary calculations of thermodynamic model. According to the results obtained, it was found that the results obtained from the thermodynamic model compared with the results obtained from experiments are convergent, and may be used in actual engine designs and applications.

تجريـــد

تم تطوير نموذج محاكاة لمحرك يعمل وفقاً لدورة اوتو اللاعكوسية وذلك باستخدام طريقة الحركيات الحرارية محدودة الزمن مع الأخذ بعين الاعتبار التغير في قيم السعات الحرارية بالنسبة للمادة العاملة تبعاً للتغير في قيم درجات الحرارة. ثلاثة عوامل مختلفة تؤثر على المحرك تمت مناقشتها، وهي: اللاعكوسية الداخلية، فقد الحرارة وفقد الإحتكاك. تم استخدام برنامج ماتلاب لإجراء الحسابات اللازمة للنموذج. وفقاً للنتائج التي تم الحصول عليها تبين أن النتائج التي تم الحصول عليها من هذا النموذج مقارنة مع النتائج التي يتم الحصول عليها من التجارب المعملية متقاربة وبالتالي يمكن استخدام هذه النتائج مستقبلاً في تصميم المحرك وتطبيقاته المختلفة.

Table of contents

List of Symbols

Symbol	Function	Unit
B	Heat leakage coefficient of the cylinder wall	kJ/kg.K
C_p	The constant pressure specific heat	kJ/kg.K
C_v	The constant volume specific heat	kJ/kg.K
D	The diffusion coefficient	m^2/s
F_μ	The friction force	N
η_I	First law efficiency	%
η_{II}	Second law efficiency	%
η_c	Compression efficiency	%
η_e	Expansion efficiency	%
η_{th}	Thermal efficiency	%
$\eta_{th,rev}$	The maximum possible thermal efficiency	%
I	The flux of electric current	$N.m^2/C$
J	The diffusion flux	$kmol/m^2.s$
K_H	Finite heat conductance for source reservoir	kW/m.K
K_L	Finite heat conductance for sink reservoir	kW/m.K
L	Stroke length of the cylinder	m
λ	The thermal conductivity	kW/m.K
M_i	The molecular weight for component ***i***	kg/kmol
$\dot{m}$	The mass flow rate of working substance	kg/s
μ	Friction coefficient for global losses	N.s/m
N	The rotational speed of the engine	rev/s
P_μ	The friction power	kW
P_{net}	The net output power	kW
q	The heat flux	kW/m^2
$\dot{Q}_{add}$	The added heat flow-rate	kW

$\dot{Q}_{loss}$	The flow-rate of heat loss	kW
$\dot{Q}_{rej}$	The rejected heat flow-rate	kW
R	The gas constant	kJ/kg.K
R_u	The universal gas constant	kJ/kg.K
r_v	The compression ratio	%
σ_e	The electric conductivity	kg
T_1	Temperature of source thermal reservoir	K
T_2	Temperature of sink thermal reservoir	K
T_{iH}	Internal high temperature for source reservoir	K
T_{iL}	Internal low temperature for sink reservoir	K
T_H	Temperature of source thermal reservoir	K
T_L	Temperature of sink thermal reservoir	K
T_0	The average temperature of the working fluid and cylinder walls	K
v	Mean piston speed	m/s
x	Piston displacement	m
x_i	The mass fraction for component ***i***.	

List of Tables

List of Figures

CHAPTER I

INTRODUTION

CHAPTER I

INTRODUTION

1.1 RESEARCH OVERVIEW

Internal combustion engines are the one of most important engines in practical life due to the board usage in various fields. Exact study and analysis for internal combustion engines is complex and the accurate analysis can be obtained experimentally when it will be carried out correctly and systematically. This would be very expensive and time-consuming. In addition, the theoretical analysis is the alternative option to study the work of the engine without the need to conduct laboratory experiments. More ever, theoretical analysis involves modeling and simulating of the engine operation with the help of thermodynamics to form mathematical expressions which is solved in order to obtain the relevant desired output parameters. However, solving method of these equations will depend on the complexity of these equations, which in turn depends on the assumptions that have been developed for the analysis of processes in the engine. Therefore more assumptions mean facilitate the solution of these equations, but in this case would be less accurate analysis.

Air standard cycle is often used as ideal cycle for internal combustion engine. In that case, air is assumed to be as an ideal gas, and all processes are considered to be reversible, there is no losses from system to the surroundings, specific heats of gas are also kept constant though they change with temperatures. But actually the working substance in the engine is not only air, it’s a mixture of fuel and air and cannot be considered as an ideal gas; as well the impossible existence of reversible processes in the engine; as result of the presence of losses due to friction. Many researchers have worked on analysis of irreversible processes in internal combustion engines which include various losses with some assumptions.

There are three main standard air cycles used for analyzing the reciprocating internal combustion engines: Diesel cycle, Otto cycle and dual cycle. Otto cycle is an idealized thermodynamic cycle that describes the functioning of a typical spark ignition piston engine. The Otto cycle was selected to be the field of study in this research.

1.2 RESEARCH PROBLEM

Problem of this research lays in the study the performance parameters of the engine that works according to the Otto cycle mathematically by using finite time thermodynamics method taking into account the specific heat variation of the working fluid with temperature.

1.3 RESEARCH IMPORTANCE

Importance of this research lies in that a mathematical analysis of the engine performance does not consume time as it is cheap contrary to experiments.

1.4 RESEARCH OBJECTIVES

- ✓ To investigate mathematically the engine performance by using finite time thermodynamics and compare these results with those obtained by experiments.
- ✓ To Study the effect of specific heat variation in the engine performance.

1.5 RESEARCH APPROACH

- ✓ This research will depend mainly on mathematical analysis.

1.6 METHODOLOGY

- ✓ Model formulation of Otto cycle by prepares all the required equations for Otto cycle that includes equations that show the relationship between the specific heat and temperature.
- ✓ Drafting a computer program using MATLAB software to solve equations of the model is to rely on iteration in this program, so that given initial values of temperatures and other parameters to run the program.
- ✓ Taking the final values obtained from the program after making sure to check the accuracy in these values, these values are plotted in order to facilitate analysis.

1.7 ANTICIPATED RESULTS

- ✓ Using the results obtained from this research in the actual design of the engine.
- ✓ Identify the thermodynamic procedures that occur inside the engine better.

1.8 THESIS LAYOUT

- ✓ **Chapter Two:** Illustrates the theoretical framework or the topics related to finite-time thermodynamics. Review the previous studies about finite-time thermodynamics and its applications in various thermodynamics cycles.
- ✓ **Chapter Three:** Shows the required equations for the thermodynamic model for Otto cycle considering the variability of specific heats for working fluid.
- ✓ **Chapter Four:** Discussion of the obtained results from the thermodynamic model illustrated in chapter three.
- ✓ **Chapter Five:** Concludes the final results and the research outputs leading to recommendations on the validity of results to be used in the engine design.

CHAPTER II

THEORETICAL BACKGROUND AND LITERATURE REVIEW

CHAPTER II

THEORETICAL BACKGROUND AND LITERATURE REVIEW

2.1 CLASSICAL EQUILIBRIUM THERMODYNAMICS

Classical Equilibrium Thermodynamics (CET) is the systematic study of transformations of matter and energy in systems in terms of a concept called thermodynamic equilibrium. The word equilibrium implies a state of balance. Equilibrium thermodynamics, in origins, derives from analysis of the Carnot cycle. Here, typically a system, as cylinder of gas, initially in its own state of internal thermodynamic equilibrium, is set out of balance via heat input from a combustion reaction. Then, through a series of steps, as the system settles into its final equilibrium state, work is extracted.

In an equilibrium state the potentials, or driving forces, within the system, are in exact balance. A central aim in equilibrium thermodynamics is: given a system in a well-defined initial state of thermodynamic equilibrium, subject to accurately specified constraints, to calculate, when the constraints are changed by an externally imposed intervention, what the state of the system will be once it has reached a new equilibrium. An equilibrium state is mathematically ascertained by seeking the extreme of a thermodynamic potential function, whose nature depends on the constraints imposed on the system. For example, a chemical reaction at constant temperature and pressure will reach equilibrium at a minimum of its components' Gibbs free energy and a maximum of their entropy.

Classical equilibrium thermodynamics differs from non-equilibrium thermodynamics, in that, with the latter, the state of the system under investigation will typically not be uniform but will vary locally in those as energy, entropy, and temperature distributions as gradients are imposed by dissipative thermodynamic fluxes. In equilibrium thermodynamics, by contrast, the state of the system will be considered uniform throughout, defined macroscopically by such quantities as temperature, pressure, or volume. Systems are studied in terms of change from one equilibrium state to another; such a change is called a thermodynamic process.

2.2 FIRST LAW EFFICIENCY

The first law of thermodynamics, also known as the conservation of energy principle, provides a sound basis for studying the relationships among the various forms of energy and energy interactions. Based on experimental observations, the first law of thermodynamics states that energy can be neither created nor destroyed during a process; it can only change forms. Therefore, every bit of energy should be accounted for during a process

First law efficiency or known as Carnot efficiency is one of the important factors for evaluating the performance of heat engines. It represents Carnot cycle efficiency.

First law efficiency determined by the following equation:

$$\eta_I = 1 - \frac{T_2}{T_1} \qquad \ldots\ldots\ldots\ldots\ldots\ldots\ldots\ldots\ldots\ldots\ldots\ldots\ldots\ldots\ldots\ldots\ldots (2.1)$$

Where:

$\boldsymbol{T_1}$ ≡ Temperature of source thermal reservoir (**K**).

$\boldsymbol{T_2}$ ≡ Temperature of sink thermal reservoir (**K**).

The above equation represents the efficiency of Carnot heat engine is the best known reversible engine. This is the highest efficiency a heat engine operating between the two thermal energy reservoirs at temperatures T1 and T2 can have.

All irreversible (i.e. actual) heat engines operating between these temperature limits (T1 and T2) have lower efficiencies. An actual heat engine cannot reach this maximum theoretical efficiency value because it is impossible to completely eliminate all the irreversibilities associated with the actual cycle.

The thermal efficiencies of actual and reversible heat engines operating between the same temperature limits compare as follows:

$$\eta_{th} \begin{cases} < \ \eta_I & irreversible\ heat\ engine \\ = \ \eta_I & revesible\ heat\ engine \\ > \ \eta_I & impossible\ heat\ engine \end{cases} \qquad \ldots\ldots\ldots\ldots\ldots\ldots\ldots\ldots\ldots\ldots\ldots\ldots\ldots\ldots\ldots (2.2)$$

2.3 SECOND LAW EFFICIENCY

The use of the second law of thermodynamics is not limited to identifying the direction of processes, however. The second law also asserts that energy has quality as

well as quantity. The first law is concerned with the quantity of energy and the transformations of energy from one form to another with no regard to its quality. Preserving the quality of energy is a major concern to engineers, and the second law provides the necessary means to determine the quality as well as the degree of degradation of energy during a process. As discussed later in this chapter, more of high-temperature energy can be converted to work, and thus it has a higher quality than the same amount of energy at a lower temperature. The second law of thermodynamics is also used in determining the theoretical limits for the performance of commonly used engineering systems, such as heat engines and refrigerators, as well as predicting the degree of completion of chemical reactions.

Second-law efficiency (also known as the exergy efficiency or rational efficiency) computes the efficiency of a process taking the second law of thermodynamics into account, is defined as the ratio of the actual thermal efficiency to the maximum possible (reversible) thermal efficiency under the same conditions

$$\eta_{II} = \frac{\eta_{th}}{\eta_{th,rev}} \quad \ldots\ldots\ldots\ldots\ldots\ldots\ldots\ldots\ldots\ldots\ldots\ldots\ldots\ldots\ldots\ldots\ldots\ldots\ldots\ldots\ldots\ldots\ldots\ldots\ldots\ldots (2.3)$$

Where:

$\boldsymbol{\eta_{th}}$ ≡ The actual thermal efficiency.

$\boldsymbol{\eta_{th,rev}}$ ≡ The maximum possible (reversible) thermal efficiency.

The destruction of exergy is closely related to the creation of entropy and as such any system containing highly irreversible processes will have low energy efficiency. As an example the combustion process inside a power stations gas turbine is highly irreversible and approximately 25% of the exergy input will be destroyed here.

2.4 NON-EQUILIBRIUM THEORY

Non-equilibrium thermodynamics borrows most of the concepts and tools from equilibrium thermodynamics but transposed at a local scale because non-equilibrium states are usually inhomogeneous. The objective is to cope with non-equilibrium situations where basic physical quantities like mass, temperature, pressure, etc. are not only allowed to change from place to place, but also in the course of time. This theory has been very useful in dealing with a wide variety of practical problems.

The relevance of transport equations, which play a central role in non-equilibrium thermodynamics - comparable, in some way, to equations of state in equilibrium thermodynamics - justifies some preliminary considerations. Transport equations describe the amount of heat, mass, electrical charge, or other quantities which are transferred per unit time between different systems and different regions of a system as a response to non-homogeneity in temperature T, molar concentration c, electric potential φ_e. Historically, the first incursions into this subject are allotted to Fourier, Fick, and Ohm, who proposed the nowadays well-known laws:

$$q = -\lambda \nabla T \quad (Fourier's\ law) \qquad \ldots\ldots\ldots\ldots\ldots\ldots\ldots\ldots\ldots\ldots (2.4)$$

$$J = -D \nabla c \quad (Fick's\ law) \qquad \ldots\ldots\ldots\ldots\ldots\ldots\ldots\ldots\ldots\ldots (2.5)$$

$$I = \sigma_e \nabla \varphi_e \quad (Ohm's\ law) \qquad \ldots\ldots\ldots\ldots\ldots\ldots\ldots\ldots\ldots\ldots (2.6)$$

Where

$\boldsymbol{q}$ ≡ The heat flux (amount of internal energy per unit time and unit area transported by conduction).

$\boldsymbol{J}$ ≡ The diffusion flux (amount of matter, expressed in moles, per unit time and unit area transported by diffusion).

$\boldsymbol{I}$ ≡ The flux of electric current (electric charge transported per unit time and unit area).

$\lambda, D\ and\ \sigma_e$ ≡ The heat transfer coefficient, diffusion coefficient, and electric conductivity, respectively.

The knowledge of these various transport coefficients in terms of temperature, pressure, and mass concentration has important consequences in material sciences and more generally on our everyday life.

2.5 REVERSIBLITY AND IRREVERSIBLITY

The second law of thermodynamics shows that there is no heat engine can have a thermal efficiency of 100%. The highest thermal efficiency is the efficiency of the Carnot cycle which consists of ideal processes or that so-called “reversible processes”.

A reversible process is defined as a process that can be reversed without leaving any trace on the surroundings. That is, both the system and the surroundings are returned to their initial states at the end of the reverse process. This is possible only if the net heat and net work exchange between the system and the surroundings is zero for the combined (original and reverse) process. As well as the reversible process can be

defined as the process that occurs it changes in some properties of the system without entropy production (i.e. dissipation of energy).

The second law of thermodynamics often leads to expressions that involve inequalities. An irreversible (i.e., actual) heat engine, for example, is less efficient than a reversible one operating between the same two thermal energy reservoirs. Another important inequality that has major consequences in thermodynamics is the Clausius inequality. It was first stated by the German physicist R. J. E. Clausius (1822–1888), one of the founders of thermodynamics, and is expressed as:

$$\oint \frac{\delta Q}{T} \leq 0 \qquad \ldots\ldots\ldots\ldots\ldots\ldots (2.7)$$

That is, the cyclic integral of dQ/T is always less than or equal to zero. This inequality is valid for all cycles, reversible or irreversible. Any heat transfer to or from a system can be considered to consist of differential amounts of heat transfer. Then the cyclic integral of dQ/T can be viewed as the sum of all these differential amounts of heat transfer divided by the temperature at the boundary.

2.6 IRREVERSIBLITIES

The factors that cause a process to be irreversible are called irreversibilities. They include friction, unrestrained expansion, mixing of two fluids, heat transfer across a finite temperature difference, electric resistance, inelastic deformation of solids, and chemical reactions. The presence of any of these effects renders a process irreversible. A reversible process involves none of these. Some of the frequently encountered irreversibilities are discussed briefly below.

Friction is a familiar form of irreversibility associated with bodies in motion. When two bodies in contact are forced to move relative to each other (a piston in a cylinder, for example, as shown in Fig. 2.1), a friction force that opposes the motion develops at the interface of these two bodies, and some work is needed to overcome this friction force. The energy supplied as work is eventually converted to heat during the process and is transferred to the bodies in contact, as evidenced by a temperature rise at the interface. When the direction of the motion is reversed, the bodies are restored to their original position, but the interface does not cool, and heat is not converted back to work. Instead, more of the work is converted to heat while overcoming the friction

forces that also oppose the reverse motion. Since the system (the moving bodies) and the surroundings cannot be returned to their original states, this process is irreversible. Therefore, any process that involves friction is irreversible. The larger the friction forces involved, the more irreversible the process is

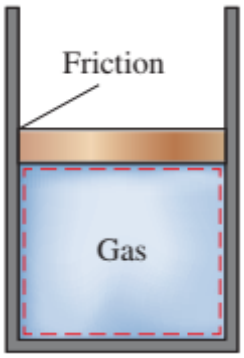

Fig. 2.1: Friction between piston and cylinder walls cause irreversible process (Cengel Y. A., Boles M. A., 2015).

Friction does not always involve two solid bodies in contact. It is also encountered between a fluid and solid and even between the layers of a fluid moving at different velocities. A considerable fraction of the power produced by a car engine is used to overcome the friction (the drag force) between the air and the external surfaces of the car, and it eventually becomes part of the internal energy of the air. It is not possible to reverse this process and recover that lost power, even though doing so would not violate the conservation of energy principle

Another example of irreversibility is the unrestrained expansion of a gas separated from a vacuum by a membrane, as shown in Fig. 2.2.

Fig. 2.2: Unrestrained expansion (Cengel Y. A., Boles M. A., 2015).

When the membrane is ruptured, the gas fills the entire tank. The only way to restore the system to its original state is to compress it to its initial volume, while transferring heat from the gas until it reaches its initial temperature. From the

conservation of energy considerations, it can easily be shown that the amount of heat transferred from the gas equals the amount of work done on the gas by the surroundings. The restoration of the surroundings involves conversion of this heat completely to work, which would violate the second law. Therefore, unrestrained expansion of a gas is an irreversible process.

A third form of irreversibility familiar to us all is heat transfer through a finite temperature difference. Consider a can of cold soda left in a warm room, as shown in Fig. 2.3.

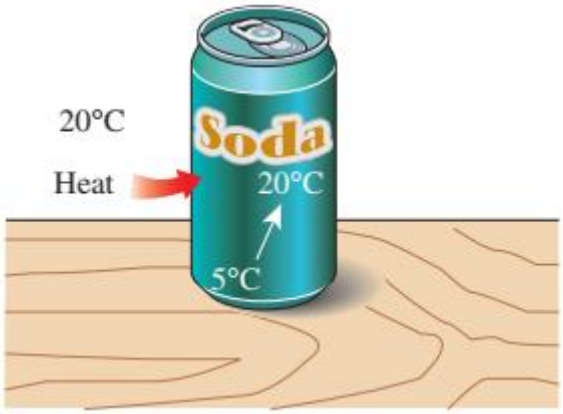

Fig. 2.3 Heat transfer through a finite temperature difference
(Cengel Y. A., Boles M. A., 2015).

Heat is transferred from the warmer room air to the cooler soda. The only way this process can be reversed and the soda restored to its original temperature is to provide refrigeration, which requires some work input. At the end of the reverse process, the soda will be restored to its initial state, but the surroundings will not be. The internal energy of the surroundings will increase by an amount equal in magnitude to the work supplied to the refrigerator. The restoration of the surroundings to the initial state can be done only by converting this excess internal energy completely to work, which is impossible to do without violating the second law. Since only the system, not both the system and the surroundings, can be restored to its initial condition, heat transfer through a finite temperature difference is an irreversible process.

2.7 ENDOREVERSIBLE THERMODYNAMICS

Reversible thermodynamic processes are convenient abstractions of real processes, which are always irreversible. Approaching the reversible regime means to become more and more quasistatic, letting behind processes which achieve any kind of finite

transformation rate for the quantities studied. On the other hand studying processes with finite transformation rates means to deal with irreversibilities and in many cases these irreversibilities must be included in a realistic description of such processes. Endoreversible thermodynamics is a non-equilibrium approach in this direction by viewing a system as a network of internally reversible (endoreversible) subsystems exchanging energy in an irreversible fashion.

Endoreversible thermodynamics is a theory for the description of irreversible thermodynamic processes. In this theory a non-equilibrium system is divided into a set of reversible subsystems which interact irreversibly with one another by exchanging energy and extensive quantities. These extensities act as carriers for the energy. ETA-Graphics is a graphics-based interface to endoreversible thermodynamics that can be used as an educational aid. It enables students to visually design endoreversible systems by drawing reversible subsystems and connecting them with irreversible (or reversible) interactions. Through special dialogs users specify the properties of the system, e.g., in form of transport laws for energy and extensive quantities. Based on the input ETA-Graphics allows students to analyse the endoreversible systems and their properties. Therefore, performance measures, i.e., efficiency and total power output, are calculated

With the development of endoreversible thermodynamics, a theory for the description of irreversible processes emerged. In this theory non-equilibrium systems are divided into sets of reversible subsystems which interact with one another by exchanging energy and extensive quantities that act as carriers for the energy. All the irreversibilities occur in the interactions between the subsystems. Thus for the subsystems themselves all the powerful tools and techniques of conventional equilibrium thermodynamics can be used, while at the same time dissipative processes are no longer neglected.

All energy transformation processes occurring in reality are irreversible and in many cases these irreversibilities must be included in a realistic description of such processes. Endoreversible thermodynamics is a non-equilibrium approach in this direction by viewing a system as a network of internally reversible (endoreversible) subsystems exchanging energy in an irreversible fashion. All irreversibilities are confined to the interaction between the subsystems. This review is dedicated to the dynamical investigation of such endoreversible systems. First the general framework for

the endoreversible description of a system is briefly introduced, and then the necessary mathematical tools to determine optimal process paths for such systems are presented. These are complemented by simple examples for the application of the different methods. Then the optimal paths for endoreversible processes of increasing complexity are discussed: first the processes between given equilibrium states, and then cyclic processes. These are followed by a review of internal combustion engines and by a number of further selected applications. We conclude with an outlook to other areas of irreversible thermodynamics where path optimization methods have been successfully used.

2.8 ENDOREVERSIBLE SYSTEM (NOVIKOV ENGINE)

An endoreversible system consists of a number of subsystems which interact with each other and with their surroundings. We choose the subsystems so as to insure that each one undergoes only reversible processes. All the dissipation or irreversibility occurs in the interactions between the subsystems or the surroundings. An endoreversible system is thus defined by the properties of its subsystems and of its interactions, (Hoffamann K. H. 2008). This process of such systems called endoreversible process. For a given thermodynamic system, the choice of an appropriate subdivision into subsystems depends on what relaxation processes are included in the dissipation, i.e. depending on what is considered a reversible process. Very often the reparability of relaxation time scales inside the composite system allows dining the subsystems in a natural way: the relaxation processes inside each subsystem must be fast compared to the rates of relaxation between subsystems, i.e. the interactions between subsystems. However, one should note that slow or fast relaxation is not equivalent to strong or weak dissipation, so once again the dining property of an endoreversible system is that all subsystems undergo only reversible processes.

As a simple introductory example we consider the Novikov engine, this engine as shown in Fig. 2.4 is a continuously operating, reversible Carnot engine with the internal temperatures T_{iH} and T_{iL}. It is in direct contact with the external low temperature heat bath at T_L and is coupled to an external high temperature heat bath at T_H through a finite heat conductance K.

One of the assumptions they made was Newtonian heat conductance, i.e. the linear dependence of heat flux on the temperature difference between sink (source) and

the working material. According to (F. L. Curzon and B. Ahlborn, (1975), if the input energy during the isothermal expansion stage is q_H, it lasts for t_1 seconds, the temperature of the working material is T_{iH}, and K_H is a constant then:

$$q_H = K_H t_1 (T_H - T_{iH}) \quad \ldots\ldots\ldots\ldots\ldots\ldots\ldots (2.8)$$

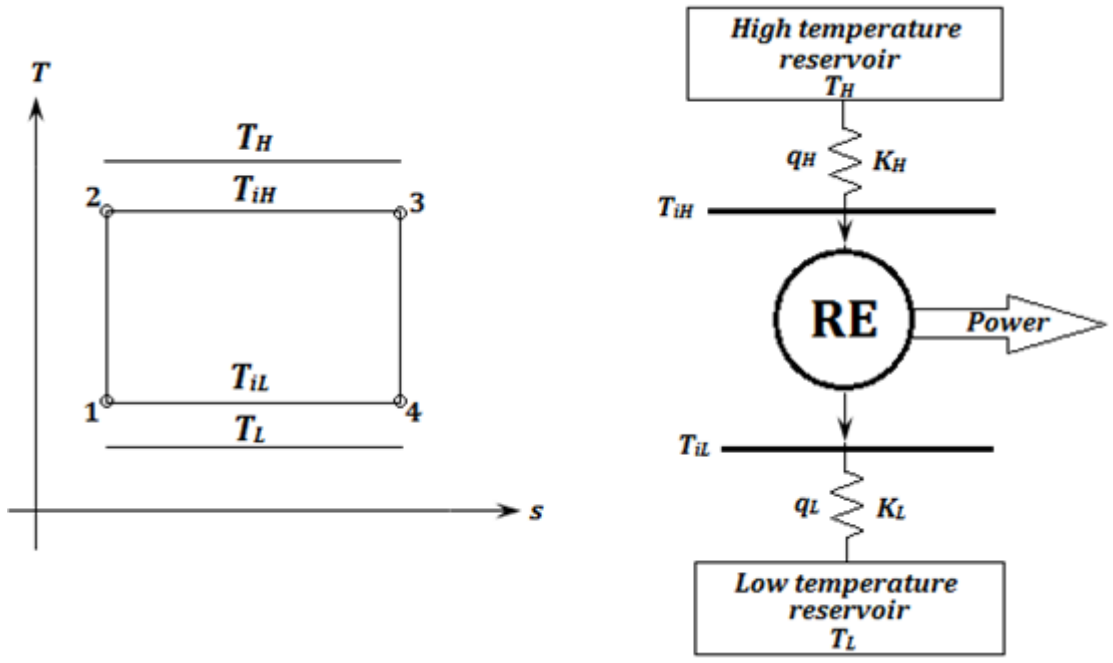

a b

Fig. 2.4 Model of the endoreversible Novicov engine with finite heat conduction K_H to the high temperature thermal reservoir and finite heat conduction K_L to the low temperature thermal reservoir (*b*).
T- s diagram of a Carnot cycle with a temperature difference to the high temperature and low temperature thermal reservoir (*a*).

Similarly, for the isothermal compression stage with the output energy q_L, duration t_2, the temperature of the working material T_{iL}, and the constant K_L we have

$$q_L = K_L t_2 (T_{iL} - T_L) \quad \ldots\ldots\ldots\ldots\ldots\ldots\ldots\ldots\ldots\ldots\ldots\ldots (2.9)$$

In addition, as the engine operates reversibly the entropy fluxes to and from the engine have to cancel

$$0 = \frac{q_H}{T_{iH}} - \frac{q_L}{T_{iL}} \rightarrow \frac{q_H}{T_{iH}} = \frac{q_L}{T_{iL}} \ldots\ldots\ldots\ldots\ldots\ldots\ldots\ldots\ldots\ldots\ldots\ldots\ldots (2.10)$$

If the total cycle duration is proportional to isothermal stages duration with constant γ, the output power of the engine is:

$$P = \frac{q_H - q_L}{\gamma(t_1 + t_2)} \quad \ldots\ldots\ldots\ldots\ldots\ldots\ldots\ldots\ldots\ldots\ldots\ldots\ldots\ldots\ldots\ldots\ldots\ldots\ldots\ldots\ldots\ldots\ldots\ldots \ (2.11)$$

Assuming that $x = T_H - T_{iH}$ and $y = T_{iL} - T_L$, the previous four equations together give:

$$P = \frac{K_H K_L xy(T_H - T_L - x - y)}{\gamma\big(K_L T_H y + K_H T_L x + xy(K_H - K_L)\big)} \quad \ldots\ldots\ldots\ldots\ldots\ldots\ldots\ldots\ldots\ldots\ldots\ldots \ (2.12)$$

The output power reaches its maximum when ∂P/∂x = ∂P/∂y = 0. These conditions lead to:

$$\left.\begin{aligned} K_L T_H y(T_H - T_L - x - y) &= x\big(K_L T_H y + K_H T_L x + xy(K_H - K_L)\big) \\ K_H T_L x(T_H - T_L - x - y) &= y\big(K_L T_H y + K_H T_L x + xy(K_H - K_L)\big) \end{aligned}\right\} \quad \begin{aligned} &\ldots\ldots\ldots (2.13a) \\ &\ldots\ldots\ldots (2.13b) \end{aligned}$$

From these two equations we than have:

$$y = \sqrt{\frac{K_H T_L}{K_L T_H}}\, x \quad \ldots\ldots\ldots\ldots\ldots\ldots\ldots\ldots\ldots\ldots\ldots\ldots\ldots\ldots\ldots\ldots\ldots\ldots\ldots\ldots\ldots\ldots\ldots\ldots\ldots\ldots \ (2.14)$$

Which is then used to eliminate $\boldsymbol{y}$ from equation (3 – 13a) to give the following quadratic equation for $\frac{\boldsymbol{x}}{\boldsymbol{T_H}} = \boldsymbol{\mu}$.

$$\left[1 - \frac{K_H}{K_L}\right]\mu^2 - 2\left[\sqrt{\frac{K_H T_L}{K_L T_H}} + 1\right]\mu + \left[1 - \frac{T_L}{T_H}\right] = 0 \quad \ldots\ldots\ldots\ldots\ldots\ldots\ldots\ldots\ldots\ldots\ldots\ldots \ (2.15)$$

Since $\boldsymbol{\mu} < 1$ the physically relevant solution of this equation is readily shown to be:

$$\mu = \frac{x}{T_H} = \frac{1 - \sqrt{T_L/T_H}}{1 + \sqrt{K_H/K_L}} \quad \ldots\ldots\ldots\ldots\ldots\ldots\ldots\ldots\ldots\ldots\ldots\ldots\ldots\ldots\ldots\ldots\ldots\ldots\ldots\ldots\ldots \ (2.16)$$

From equation (3 – 14) it follows that

$$\frac{y}{T_L} = \frac{\sqrt{T_H/T_L} - 1}{1 + \sqrt{K_L/K_H}} \quad \ldots\ldots\ldots\ldots\ldots\ldots\ldots\ldots\ldots\ldots\ldots\ldots\ldots\ldots\ldots\ldots\ldots\ldots\ldots\ldots\ldots\ldots \ (2.17)$$

The efficiency of the engine at maximum power ($\boldsymbol{\eta_{Pmax}}$) is given by:

$$\eta_{Pmax} = 1 - \frac{T_{iL}}{T_{iH}} = 1 - \frac{T_L + y}{T_H - x} \quad \ldots\ldots\ldots\ldots\ldots\ldots\ldots\ldots\ldots\ldots\ldots\ldots\ldots\ldots\ldots\ldots\ldots \ (2.18)$$

By substituting $\boldsymbol{x}$ and $\boldsymbol{y}$ in equation (3 – 18) we get:

$$\eta_{Pmax} = 1 - \sqrt{\frac{T_L}{T_H}} \quad \ldots\ldots\ldots\ldots\ldots\ldots\ldots\ldots\ldots\ldots\ldots\ldots\ldots\ldots\ldots\ldots\ldots\ldots\ldots\ldots\ldots\ldots\ldots \ (2.19)$$

The efficiency in equation (2 – 19) is called Novicov's efficiency.

2.9 HISTORICAL BACKGROUND

Finite-time thermodynamics was 'invented' in 1975 by R. S. Berry, P. Salamon, and B. Andersen as a consequence of the first world oil crisis. It simply dawned on us that all the existing criteria of merit were based on reversible processes and therefore were totally unrealistic for most real processes. That made an evaluation of the potential for improvement, of minimizing the losses, for a given process quite difficult. Finite-time thermodynamics is coming of age. A child of the 1973 oil crisis, it was conceived in 1975, and the first publication on this topic appeared in 1977.

Badescu and Andresen proposed that finite-time thermodynamics (F.T.T.) can be complemented with some probabilistic concepts allowing a more accurate description of the performance indicators of a power system (Badescu, V., Andresen B., 1996). They studied a continuous flow tube reactor which supplies heat to an engine from a chemical reaction with linear kinetics. In general, typical FTT-models of thermal cycles are worked in steady state and only one cycle is taken as representative of all the other cycles pertaining to a sequence of them. In a typical internal combustion engine, several thousands of cycles are performed in a minute and there exist theoretical and experimental reasons to expect important variations from one cycle to the next.

2.10 LITERATURE REVIEW

Angulo-Brown F. et al., (1996) proposed an irreversible simplified model for the air standard Otto thermal cycle. This model takes into account the finite-time evolution of the cycle's compression and power strokes and it considers global losses lumped in a friction like term. The proposed model permits the maximization of quantities such as the power output and the efficiency in terms of the compression ratio r_v. The optimum r_v values obtained compare well with standard r_v values for real Otto engines. This model leads to loop-shaped power-versus-efficiency curves as is common to almost all real heat engines.

Hernandez A. C. et al., (1995) presented a simplified model for an irreversible Otto cycle which accounts for the characteristic power-versus-efficiency curve of real heat engines. This model avoids the usual hypotheses of endoreversible heat engines

and it considers an air Otto engine with internally dissipative friction and a pure sinusoidal law for the piston velocity on the adiabatic branches.

Angulo-Browndag F. et al., (1994) proposed a finite-time thermodynamics model for an Otto thermal cycle. This model considers global losses in a simplified way lumped into a friction-like term, and takes into account the departure from an endoreversible regime through a parameter (R) arising from the Clausius inequality. The numerical results suggest that the cycle's power output and efficiency are very sensitive to that parameter. It found that R is the ratio of the constant-volume heat capacities of the reactants and products in the combustion reaction occurring inside the working fluid. The results have implications in the search for new fuels for internal combustion engines.

Angulo-Brown F et al., (1996) proposed an irreversible simplified model for the air standard Otto thermal cycle. This model takes into account the finite-time evolution of the cycle's compression and power strokes and it considers global losses lumped in a friction like term. The proposed model permits the maximization of quantities such as the power output and the efficiency in terms of the compression ratio r_v. The optimum r_v values obtained compare well with standard r_v values for real Otto engines. This model leads to loop-shaped power-versus-efficiency curves as is common to almost all real heat engines.

Noam Lior (1998) calculated for compression ratios of 3.0:9.0 and air/fuel equivalence ratios of 0.25:1.0 the system input and output exergy at each portion of an ideal Otto cycle, as well as the process effectiveness, are calculated for compression ratios of 3.0:9.0 and air/fuel equivalence ratios of 0.25:1.0. For comparison, the energy-based efficiencies are also calculated. It was found that both effectiveness and efficiency increase with compression ratio and with air-to-fuel ratio (but at different rates), and that the effectiveness does not vary much when the air-to-fuel ratio increases above 200%. It was also shown that exergy analysis represents the losses in the cycle, such as in the combustion and exhaust processes, much more realistically than the conventional first-law analysis and serves as a good guide for cycle improvements. Several recommendations are made in that direction.

Lingen Chen (1998) performed finite-time thermodynamic analysis of an air-standard Otto cycle. The relation between net work output and efficiency of the cycle is derived. The maximum net work output and the corresponding efficiency bound of the cycle with heat transfer considerations are also found. Detailed numerical examples are given. The result obtained herein provides a guide to the performance evaluation and improvement for practical Otto engines.

The concept of the efficiency of a process is used to analyse various thermodynamic power cycles with ideal gases, Aragón-González G et al., (2000). The Otto cycle is treated by considering irreversibilities coming exclusively from expansion and compression processes. For this cycle, the maximum irreversible work and the maximum efficiency are obtained in terms of the isentropic efficiencies and of the maximum and minimum temperatures of the reversible cycle. The results obtained are easily applicable to the Brayton cycle and have some similarities with those obtained from finite-time thermodynamics. The expression found for the efficiency of the Otto cycle for irreversible maximum work is similar to that obtained by maximizing the irreversible work in the Curzon-Ahlborn-Nokivov engine.

One of the major alternatives of the Otto cycle has been examined to determine its potential for increased efficiency and net work power in the spark ignited internal combustion engine is to shorten the compression process relative to the expansion process by early close or late of intake valve, Chin Wu (2000). The modified Otto cycle is called Miller cycle. This work deals with the analysis of a supercharged Otto engine adopted for Miller cycle operation. The Miller cycle shows no efficiency advantage and suffers a penalty in power output in the normally aspirated version. In the supercharged Otto engine adopted for Miller cycle version, it has no efficiency advantage but does provide increased net work output with reduced propensity to engine knock problem. Sensitivity analysis of cycle efficiency versus early close of intake valve and that of cycle net work versus early close of intake valve are performed. Optimization on the cycle efficiency is obtained.

The performance of an air-standard Otto cycle with heat transfer loss and variable specific heats of working fluid is analyzed by using finite-time thermodynamics, (Ge Yanlin, et al., 2005). The relations between the power output and the compression ratio, between the thermal efficiency and the compression ratio, as well

as the optimal relation between power output and the efficiency of the cycle are derived by detailed numerical examples. Moreover, the effects of heat transfer loss and variable specific heats of working fluid on the cycle performance are analyzed. The results show that the effects of heat transfer loss and variable specific heats of working fluid on the cycle performance are obvious, and they should be considered in practice cycle analysis. The results obtained in this paper may provide guidance for the design of practice internal combustion engines.

The model of an irreversible Otto cycle using an ideal Fermi gas as the working fluid, which is called as the irreversible Fermi Otto cycle, is established by Feng Wu, Lingen et al., (2005). Based on the equation of state of an ideal Fermi gas, the ecological optimization performance of an irreversible Fermi Otto cycle is examined by taking an ecological optimization criterion as the objective, which consists of maximizing a function representing the best compromise between the exergy output and exergy loss (entropy production) of the cycle. The relationship between the ecological function E and the efficiency η is studied. Three special cases are discussed in detail. The results obtained herein may reveal the general performance characteristics of the irreversible Fermi Otto cycle.

Shuhn-Shyumg Hou (2007) studied the effects of heat transfer on the net output work and the indicated thermal efficiency of an air standard Atkinson cycle is analyzed. Comparisons of the performances of air standard Atkinson and Otto cycles with heat transfer considerations are also discussed. We assume that the compression and power processes are adiabatic and reversible and that any convective, conductive or radiative heat transfer to the cylinder wall during the heat rejection process may be ignored. The heat loss through the cylinder wall is assumed to occur only during combustion and is further assumed to be proportional to the average temperature of both the working fluid and cylinder wall. It is found that the net output work versus efficiency characteristics, the maximum net work output and the corresponding efficiency bound are significantly influenced by the magnitude of the heat transfer. An increase in heat transfer to the combustion chamber walls decreases the peak temperature and pressure and, consequently, reduces the work per cycle and efficiency. The effects of other parameters, in conjunction with heat transfer, including combustion constants, compression ratio and intake air temperature are also reported. An Atkinson cycle has a

greater work output and a higher thermal efficiency than the Otto cycle at the same operating condition. The compression ratios that maximize the work of the Otto cycle are always found to be higher than those for the Atkinson cycle at the same operating conditions. The results are of importance to provide good guidance for performance evaluation and improvement of practical Atkinson engines

The performance of an air standard Otto-cycle is analyzed using finite-time thermodynamics (Ge Yanlin, et al., 2008). In the irreversible cycle model, the non-linear relation between the specific heat of the working fluid and its temperature, the friction loss computed according to the mean velocity of the piston, the internal irreversibility described by using the compression and expansion efficiencies, and the heat-transfer loss are considered. The relations between the power output and the compression ratio, between the thermal efficiency and the compression ratio, as well as the optimal relation between the power output and the efficiency of the cycle are indicated by numerical examples. Moreover, the effects of internal irreversibility, heat-transfer loss and friction loss on the cycle performance are analyzed. The results obtained in this paper may provide guidance for the design of practical internal-combustion engines.

The objective of their work (Jiann-Changlin 2008) was to analyze the effects of heat loss characterized by a percentage of the fuel's energy, friction and variable specific heats of working fluid on the performance of an air standard Otto cycle with a restriction of maximum cycle temperature. A more realistic and precise relationship between the fuel's chemical energy and the heat leakage that is based on a pair of inequalities is derived through the resulting temperature. The variations in power output and thermal efficiency with compression ratio, and the relations between the power output and the thermal efficiency of the cycle are presented. The results show that the power output as well as the efficiency where maximum power output occurs will increase with increase of the maximum cycle temperature. The temperature dependent specific heats of the working fluid have a significant influence on the performance. The power output and the working range of the cycle increase with the increase of specific heats of the working fluid, while the efficiency decreases with the increase of specific heats of the working fluid. The friction loss has a negative effect on the performance. Therefore, the power output and efficiency of the cycle decrease with increasing friction loss. It is noteworthy that the effects of heat loss characterized by a percentage of the

fuel's energy, friction and variable specific heats of the working fluid on the performance of an Otto cycle engine are significant and should be considered in practical cycle analysis. The results obtained in the present study are of importance to provide good guidance for performance evaluation and improvement of practical Otto engines.

The aim of their study (Barry Cullen et al., 2010) was to investigate the feasibility of utilising a Stirling cycle engine as an exhaust gas waste heat recovery device for an Otto cycle internal combustion engine (ICE) in the context of an automotive power plant. The hybrid arrangement would produce increased brake power output for a given fuel consumption rate when compared to an ICE alone. The study was dealt with from an energy system perspective with design practicalities such as power train integration, location of auxiliaries, manufacture costs and other general plant design considerations neglected. The study necessitated work in two distinct areas: experimental assessment of the performance characteristics of an existing automotive Otto cycle ICE and mathematical modelling of the Stirling cycle engine based on the output parameters of the ICE. It was subsequently found to be feasible in principle to generate approximately further 30% useful power in addition to that created by the ICE by using a Stirling cycle engine to capture waste heat expelled from the ICE exhaust gases over the complete range of engine operating speeds.

An irreversible cycle model of the micro-/nanoscaled Otto engine cycle with internal friction loss is established (Wenjie Nie, 2010). The general expressions of the work output and efficiency of the cycle are calculated based on the finite system thermodynamic theory, in which the quantum boundary effect of gas particles as working substance and the mechanical Casimir effect of gas system are considered. It is found that, for a micro-/nanoscaled Otto cycle devices, the work output W and efficiency η of the cycle can be expressed as the functions of the temperature ratio τ of the two heat reservoirs, the volume ratio r_V and the surface area ratio r_A of the two isochoric processes, the dimensionless thermal wavelength λ and other parameters of cycle, while for a macro scaled Otto cycle devices, the work output W_0 and efficiency η_0 of the cycle are independent of the surface area ratio r_A and the dimensionless thermal wavelength λ. Further, the influence of boundary of cycle on the performance characteristics of the micro-/nanoscaled Otto cycle are analyzed in detail

by introducing the output ratio W/W_0 and efficiency ratio η/η_0. The results present the general performance characteristics of a micro-/nanoscaled Otto cycle and may serve as the basis for the design of a realistic Otto cycle device in micro-/nanoscale.

Using finite-time thermodynamics (R. Ebrrahimi, 2010), the relations between the work output and the compression ratio, between the thermal efficiency and the compression ratio for an endoreversible Otto cycle are derived with variable specific heat ratio of working fluid. The results show that if compression ratio is less than certain value, the increase of specific heat ratio makes the work output and the thermal efficiency higher; on the contrary, if compression ratio exceeds certain value, the increase of specific heat ratio makes the work output and the thermal efficiency less. The results also show that the maximum work output, the compression ratio at the maximum work output point, the working range of the cycle and the compression ratio at maximum thermal efficiency point decrease as the specific heat ratio increased. The results obtained from this work can be helpful in the thermodynamic modeling and in the evaluation of real Otto engines

In their paper (Usta Y., Sahina B. et al., 2011) they reports the thermodynamic optimization based on the maximum mean effective pressure, maximum power and maximum thermal efficiency criteria for an irreversible Otto heat engine model which includes internal irreversibility resulting from the adiabatic processes. The mean effective pressure, power output, and thermal efficiency are obtained by introducing the compression ratio, cycle temperature ratio, specific heat ratio and the compression and expansion efficiencies. Optimal performance and design parameters of the Otto cycle are obtained analytically for the maximum power and maximum thermal efficiency conditions and numerically for the maximum mean effective pressure conditions. The results at maximum mean effective pressure conditions are compared with those results obtained by using the maximum power and maximum thermal efficiency criteria. The effects of the cycle temperature ratio and cycle pressure ratio on the general and optimal performances are investigated.

Levan Chotorlishvili, (2011) studied the influence of the dynamical Stark shift on the thermal entanglement and the efficiency of the quantum Otto cycle is studied for the su (1,1) Tavis–Cummings system. It is shown that the degree of the thermal entanglement becomes larger as the dynamical Stark shift increases. In contrast, the

efficiency of the Otto cycle is degraded with an increase of the values of the dynamical Stark shift. Expressions for the efficiency coefficient are derived. Using those expressions, they identify the maximal efficiency of the quantum Otto cycle from the experimentally measured values of the dynamical Stark shift.

Neutronic characteristics were investigated (Hoai Nam Tran et al., 2012) for a once-through-then-out (OTTO) refueling scheme based on the 400 MW pebble bed modular reactor (PBMR) and compared with that of a reference multi-pass scheme. The core was loaded with new fuel pebbles which were designed with Gd2O3 particles to flatten the axial power profile. The Gd2O3 design was considered in a multi-parameter optimization to maximize the average discharged burn up while maintaining a limited power peak and ensuring core criticality. The results show that the OTTO scheme using the new fuel pebbles can achieve the maximum average discharged burn up of about 75 GWd/t, at which the core neutronic characteristics are comparable with that of the reference multi-pass scheme. This means that the efficiency of fuel utilization of the OTTO scheme is about 21% less than that of the multi-pass scheme (95 GWd/t).

Hai Li and Jian Zou (2013) considered a single quantum mechanical particle confined to an one-dimensional (1D) infinite square well, and propose a nonequilibrium quantum Otto cycle (NQOC). Compared with the conventional quantum Otto engine (CQOE) investigated by Kieu T.D., (Kieu T.D. 2004), (Kieu T.D. 2006), due to the effects of negentropy produced in the NQOC, many interesting features appear: (1) in general, the NQOC is capable of extracting more work, so it is more efficient; (2) the NQOC can operate even when $T_1 = T_2$ or $T_1 < T_2$, where T_1 (T_2) represents the temperature of hot (cold) bath; (3) in some cases, the NQOC can absorb heat from both baths and completely transforms them into work. These results demonstrate that the negentropy can be understood as an effective source of efficiency in quantum heat engines (QHEs) and meanwhile it is shown that the second law of thermodynamics is not violated. At last, they also show that the efficiency of NQOC reduces to that of classical Otto cycle in the classical limit.

Feilong Wu et al., (2014) considered the efficiency at maximum power of a quantum Otto engine, which uses a spin or a harmonic system as its working substance and works between two heat reservoirs at constant temperatures T_h and T_c ($<T_h$). Although the behavior of spin-1/2 system differs substantially from that of the harmonic

system in that they obey two typical quantum statistics, the efficiencies at maximum power based on these two different kinds of quantum systems are bounded from the upper side by the same expression:

$$\eta_{mp} \leq \eta_+ \equiv \eta 2C/[\eta C-(1-\eta C)\ln(1-\eta C)] \text{ with } \eta C=1-Tc/Th$$

as the Carnot efficiency. This expression ηmp possesses the same universality of the CA efficiency $\eta CA=1-\sqrt{1-\eta C}$ at small relative temperature difference. Within the context of irreversible thermodynamics, they calculate the Onsager coefficients and show that the value of ηCAis indeed the upper bound of EMP for an Otto engine working in the linear-response regime.

Considering internal irreversibility loss (IIL), friction loss (FL) and heat transfer loss (HTL), an irreversible Otto cycle (IOC) model was built up by using air standard (AS) assumption (Yanlin Ge et al., 2014). Based on finite-time thermodynamics (FTT), computing entropy generation rate (EGR) by using the irreversible losses in the cycle, the ecological function (EF) performance of the cycle is optimized when the specific heat (SH) of the working fluid (WF) varies with temperature with linear relation. Some important expressions, including efficiency, power output, EGR and EF, are obtained. Moreover, the effects of variable SH of WF and three losses on cycle performance are investigated. The research conclusion can provide some guidelines for the actual Otto cycle engine performance optimization.

In recent years, numerous analyses have been performed on Otto cycles and Otto engines, but these have often yielded different output powers and engine thermal efficiencies. In their study, (Mohammad H. Ahmed et al., 2015), output power and engine thermal efficiency are optimized and entropy generation is minimized using a NSGA algorithm and thermodynamic analysis. The Pareto optimal frontier is obtained and a final optimal solution is selected using various decision-making approaches, including fuzzy Bellman-Zadeh, LINMAP and TOPSIS methods. The results enhance understanding of the performances of Otto cycles and of their optimization.

The concept of inner friction, by which a quantum heat engine is unable to follow adiabatically its strokes and thus dissipates useful energy, is illustrated in an exact physical model where the working substance consists of an ensemble of misaligned spins interacting with a magnetic field and performing the Otto cycle. (Alecce A. and

Galve F., 2015). The effect of this static disorder under a finite-time cycle gives a new perspective of the concept of inner friction under realistic settings. The efficiency and power of this engine has been investigated and relate its performance to the amount of friction from misalignment and to the temperature difference between heat baths. Finally an alternative experimental implementation of the cycle where the spin is encoded in the degree of polarization of photons was proposed.

Throughout the recent years, several efforts have been conducted in studying Stirling engine which have yielded various models for analysis of Stirling engine thermal efficiency and output power (Mohammad H. Ahmadi et al., 2016). In this study, the applicability of a combined Stirling and Otto cycle power plant where a Stirling cycle engine would serve as a bottoming cycle for a stationary Otto cycle engine is investigated. Output power of Stirling engine and Stirling engine thermal efficiency are optimized and total pressure losses of Stirling engine is optimized executing NSGA approach and finite speed thermodynamic analysis. The outcomes gained are satisfactory verified versus actual recorded data of Stirling engine. Decision making was performed via three well-known methods. Finally, error analysis was performed on the outputs obtained from this optimization.

A thermodynamic analysis for an irreversible Otto–Miller Cycle (OMC) has been presented by taking into consideration heat transfer effects, frictions, time-dependent specific heats, internal irreversibility resulting from compression and expansion processes (Erinc Dobrucali, 2016). In the analyses, the influences of the engine design parameters such as cycle temperature ratio, cycle pressure ratio, friction coefficient, engine speed, mean piston speed, stroke length, inlet temperature, inlet pressure, equivalence ratio, compression ratio, and bore-stroke length ratio on the effective power, effective power density and effective efficiency have been investigated relations with efficiency in dimensionless form. The dimensionless power output and power density and thermal efficiency relations have been computationally obtained versus the engine design parameters. The results demonstrate that the engine design and running parameters have considerable effects on the cycle thermodynamic performance of a OMC. The results showed that the cycle efficiency increased up to 50%, as cycle temperature ratio increases from 6 to 8, the effective power raised to 11 kW from 5 kW at this range. Other parameters such as engine speed, mean piston speed, cycle pressure

ratio affected the performance up to 30%, positively. However, friction coefficient and inlet temperature have negative effect on the performance. As the friction coefficient increases from 12.9 to 16.9, a performance reduction was seen up to 5%. Increase of the inlet temperature abated the performance by 40%.

In their study, (Alper Dalkiran et al., 2016), exergetic sustainability index is applied to quantum irreversible Otto cycle with -1/2 spin system. Exergetic sustainability index in a quantum engine is used first time. This index is the ratio of exergy output (work output for a thermal engine) to total exergetic losses. It gives an opportunity to evaluate for all thermodynamic losses in the system, that is why, it is an important index. In addition, some thermodynamic parameters (work output, exergy destruction, first and second law efficiencies) are considered and their relationships between the exergetic sustainability index are determined.

Mohammad H. Ahmadi et al., (2016) made attempt to investigate thermodynamically a nano-scale irreversible Otto cycle for optimizing its performance. This system employed an ideal Maxwell–Boltzmann gas as a working fluid. Two different scenarios were proposed in the multi-objective optimization process and the results of each of the scenarios were examined separately. The first scenario made attempt to maximize the dimensionless ecological function and minimize the dimensionless entransy dissipation of the system. Furthermore, the second scenario tried to maximize the ecological coefficient of performance and minimize the dimensionless entransy dissipation of the system. The multi objective evolutionary method integrated with non-dominated sorting genetic algorithm was used to optimize the proposed objective functions. To determine the final output of each scenario, three efficient decision makers were employed. Finally, error analysis was employed to determine the deviation of solutions chosen by decision makers.

In this paper, comparative performance analyses of the irreversible OMCE (Otto Miller cycle engine), DiMCE (Diesel Miller cycle engine) and DMCE (Dual Miller cycle engine) based on the MP (maximum dimensionless power) output, MPD (maximum dimensionless power density) and MEF (maximum thermal efficiency) criteria have been performed by taking irreversibility due to irreversible-adiabatic compression and expansion processes into account. The maximum values of the thermal efficiency, dimensionless power output and dimensionless power density are obtained

depending on pressure ratio, stroke ratio, cut-off ratio, miller cycle ratio, exhaust temperature ratio, cycle temperature ratio and cycle pressure ratio and the isentropic efficiencies of irreversible-adiabatic processes. The engine design parameters at the MP, MPD and MEF conditions are determined and their variations are investigated with respect to miller cycle ratio.

Edson Vanzela et al., (2017) evaluated the effect of adding different concentrations of biodiesel to ethanol, analyzing its heating value, viscosity, flash point and density. Eight different compositions were carried out (4 blends with soybean biodiesel and 4 with castor bean oil), by varying the percentage of biodiesel at 1%, 3%, 5% and 10% (m/m) hydrous ethanol. The highest heating value increase was achieved in the blend with 10% soybean biodiesel (+8.70%). The blend with 10% castor bean biodiesel showed a viscosity increase of 23.8% whereas blends with 5% castor bean oil and 10% soybean biodiesel presented a viscosity increase of 15%. The flash point for blends with 10% soybean and castor bean biodiesel increased by just over 1 °C, improving safety condition in the handling of the fuel. The density exceeded the specified limit of 1.42% for the blend with 10% castor bean oil. This parameter is dependent on the amount of water present in ethanol, which in this study achieved the maximum limit, thus making the density of the blends exceed the threshold.

The quantum Otto cycle serves as a bridge between the macroscopic world of heat engines and the quantum regime of thermal devices composed from a single element (Ronnie Kosloff et al., 2017). Compile recent studies of the quantum Otto cycle with a harmonic oscillator as a working medium. This model has the advantage that it is analytically tractable. In addition, an experimental realization has been achieved, employing a single ion in a harmonic trap. The review is embedded in the field of quantum thermodynamics and quantum open systems. The basic principles of the theory are explained by a specific example illuminating the basic definitions of work and heat. The relation between quantum observables and the state of the system is emphasized. The dynamical description of the cycle is based on a completely positive map formulated as a propagator for each stroke of the engine. Explicit solutions for these propagators are described on a vector space of quantum thermodynamically observables. These solutions which employ different assumptions and techniques are compared. The tradeoff between power and efficiency is the focal point of finite-time-

thermodynamics. The dynamical model enables the study of finite time cycles limiting time on the adiabatic and the thermalization times. Explicit finite time solutions are found which are frictionless (meaning that no coherence is generated), and are also known as shortcuts to adiabaticity. The transition from frictionless to sudden adiabats is characterized by a non-hermitian degeneracy in the propagator. In addition, the influence of noise on the control is illustrated. These results are used to close the cycles either as engines or as refrigerators. The properties of the limit cycle are described. Methods to optimize the power by controlling the thermalization time are also introduced. At high temperatures, the Novikov–Curzon–Ahlborn efficiency at maximum power is obtained. The sudden limit of the engine which allows finite power at zero cycle time is shown. The refrigerator cycle is described within the frictionless limit, with emphasis on the cooling rate when the cold bath temperature approaches zero.

Considering internal irreversibility loss (IIL), friction loss (FL) and heat transfer loss (HTL), an irreversible Otto cycle (IOC) model is built up by using air standard (AS) assumption (Yanlin Ge et al., 2017). Based on finite-time thermodynamics (FTT), computing entropy generation rate (EGR) by using the irreversible losses in the cycle, the ecological function (EF) performance of the cycle is optimized when the specific heat (SH) of the working fluid (WF) varies with temperature with linear relation. Some important expressions, including efficiency, power output, EGR and EF, are obtained. Moreover, the effects of variable SH of WF and three losses on cycle performance are investigated. The research conclusion can provide some guidelines for the actual Otto cycle engine performance optimization.

The purpose of his (Awad M. 2017) discussion is to increase the awareness of the divergent views on the entransy concept among the readers of chemical physics. Comments are presented in particular on the paper by Ahmadi et al., (2016) where the authors used entransy dissipation in their analysis. Based on the view points of independent different groups of researchers world wide, I draw the attention of readers to the reality that entransy has no physical meaning.

Selcuk Cakmak (2017) proposed an arbitrary driven spin as the working fluid of a quantum Otto cycle in the presence of internal friction. The role of total allocated time to the adiabatic branches of the cycle, generated by different control field profiles, on

the extractable work and the thermal efficiency are analyzed in detail. The internal friction is characterized by the excess entropy production and quantitatively determined by studying the closeness of an actual unitary process to an infinitely long one via quantum relative entropy. It is found that the non-ideal, finite-time adiabatic transformations negatively effect the work output and the thermal efficiency of the quantum heat engine. The non-monotone dependence of the work output, thermal efficiency, entropy production and the internal friction on the total adiabatic time are elucidated. It is also found that almost frictionless adiabatic transformations with small entropy production can be obtained in a short adiabatic time. Complete frictionless solutions for finite adiabatic times, possible implementation of our engine in NMR setups and the estimation of the power output have also been analyzed.

Santos E. M. (2017) conduct experimental trials during a research is a process that demands time and financial resources, being important the use of tools such as computer programs or theoretical calculations methodologies that allow to find results closer to the real ones, there for representing a reduction of time and cost of the research. In the development of engines, studies of the thermodynamic cycle through the pressure curve inside the cylinder are of fundamental importance for the analysis of the combustion process. This work presents an evaluative and comparativee study between the thermal calculation of an internal combustion engine, with results obtained from simulations in the Siciclo software and with results obtained from experimental tests. The thermal calculation is based on the First Law of Thermodynamics and it was developed on a spreadsheet. The Siciclo is a software developed in an academic environment, which consists of the simulation of the pressure and temperature curves inside an engine from an imposed combustion law and through solution of the First Law of Thermodynamics. The experimental tests were performed on a test bench, consisting of a single cylinder engine instrumented with a pressure transducer, a crank angle encoder and thermocouples, coupled to a hydraulic dynamometer. The pressure curve inside the combustion chamber and the external speed characteristic curve obtained by each method were compared, aiming to verify the accuracy of the theoretical and simulated results in relation to the actual results. The thermal calculation overestimated the maximum pressure by 44%, mainly due to the consideration of instantaneous combustion at constant volume, while the Siciclo, mainly by adopting the Wiebe

burning law, overestimated the maximum pressure by only 2%. From the pressure data, analyzes justifying the differences in the external speed characteristic curve were made

Considering internal irreversibility loss, friction loss and heat transfer loss, an irreversible Otto cycle model is built up by using finite-time thermodynamics with air standard assumption, (Yanlin Ge et al., (2018). Using the various irreversible losses in the cycle to compute the entropy generation rate, the optimal ecological function performance of the cycle is studied when the specific heats of working fluid are nonlinear relation with its temperature. Some important expressions, including ecological function, entropy generation rate, efficiency and power output, are obtained. The cycle ecological function performances with constant specific heats, specific heats changed with linear and nonlinear relations of its temperature are compared. Moreover, the impacts of internal irreversibility loss, friction loss and heat transfer loss on ecological function performance are analyzed. The results show that optimization of the exergy-based ecological function not only represents a compromise between the power output and the rate of entropy generation but also represents a compromise between the power output and the thermal efficiency, the specific heat models have no qualitative effect and only have quantitative effect on the performance characteristics of ecological function versus power output and ecological function versus efficiency, and the ecological function, power output and efficiency decrease with the increase of heat transfer, friction and internal irreversibility losses.

Variety of technologies along with the mechanisms for their implementations has been developed in order to pursue possible improvements in the performance and efficiency of gasoline engines, (Yangtao Li 2018). However, most of the commonly used techniques, such as the cam-based variable valve timings (VVT) and variable compression ratio (VCR), are realized by different kinds of complicated mechanisms, providing an extended but still relatively limited adjustability for attaining improved valve timings and different engine cycles according to the varying working conditions of the engine. In this research, by using the flexibility offered by the hydraulic actuated valve train (HAVT), a set of new valve motion strategies is developed for realizing a newly introduced engine cycle, the variable Otto-Atkinson cycle (VOAC), to achieve an unthrottled engine load control. The demonstrative VOAC test engine in this research is a converted baseline single-cylinder engine that is able to carry out a variable Otto cycle

(VOC) at full load operations for achieving higher power performance while realizing a variable Atkinson cycle (VAC) at partial load operations for gaining better fuel economy without having any further modifications or attaching additional components to the engine. The baseline single-cylinder engine is modeled in GT-Suite and carefully calibrated by a series of experiments. Benefited from the HAVT features, the tunings of the VOAC engine can be realized easily to fulfill any requirements towards different desired engine characteristics. By adopting the proposed VOAC with optimized parameters, a 13.5% average improvement in the engine's output can be achieved under full load operations across the entire speed range. On top of that, it also shows that the resulted BSFC could be lowered by 16.1 g/kWh on average over the sampled speed-load map of the engine running at partial load operations.

Finite-time thermodynamic models for an Otto cycle, an Atkinson cycle, an over-expansion Miller cycle (M1), an LIVC Miller cycle through late intake valve closure (M2) and an LIVC Miller cycle with constant compression ratio (M3) have been established (Jinxing Zhao et al., 2018). The models for the two LIVC Miller cycles are first developed; and the heat-transfer and friction losses are considered with the effects of real engine parameters. A comparative analysis for the energy losses and performances has been conducted. The optimum compression-ratio ranges for the efficiency and effective power are different. The comparative results of cycle performances are influenced together by the ratios of the energy losses and the cycle types. The Atkinson cycle has the maximum peak power and efficiency, but the minimum power density; and the M1 cycle can achieve the optimum comprehensive performances. The less net fuel amount and the high peak cylinder pressure (M3 cycle) have a significantly adverse effect on the loss ratios of the heat-transfer and friction of the M2 and M3 cycles; and the effective power and energy efficiency are always lower than the M1 and Atkinson cycles. When greatly reducing the weights of the heat-transfer and friction, the M3 cycle has significant advantage in the energy efficiency. The results obtained can provide guidance for selecting the cycle type and optimizing the performances of a real engine

A novel system consisting of an external heat source, a direct carbon solid oxide fuel cell (DC-SOFC), a regenerator and an air standard Otto cycle engine is proposed to improve the performance of the DC-SOFC (Haoran Xu et al., 2018). Considering the

electrochemical/chemical reactions, ionic/electronic charge transport, mass/momentum transport and heat transfer, a 2D tubular DC-SOFC model shows that the overall heat released in the cell can be smaller than, equal to or larger than the heat required by the internal Boudouard reaction. Three different operating modes of the proposed system are identified, and accordingly, analytical expressions for the equivalent power output and efficiency of the proposed system are derived under different operating conditions. The modeling results show that the Otto heat engine can effectively recover the waste heat from the DC-SOFC for additional power production especially at large operating current density. Comprehensive parametric studies are conducted to investigate the effects of the different operating conditions of DC-SOFC on its performance and heat generation. The effects of compression ratio, internal irreversibility factor and power dissipation of the Otto heat engine on the system performance improvement are also studied.

CHAPTER III

THERMODYNAMIC MODELING

CHAPTER III
THERMODYNAMIC MODELING

3.1 INTRODUCTION

This chapter will address the thermodynamic model for Otto cycle, and will take into account the change in the specific heat values of the working substance due to change in temperature. Will use MATLAB software to create a program to conduct the thermodynamic model calculations, and then we will present the results that will be obtained when we execute the program.

3.2 OTTO ENGINE THERMODYNAMIC CYCLE MODEL

An air standard Otto-cycle model is shown in Fig. 3.1 in T-s diagram.

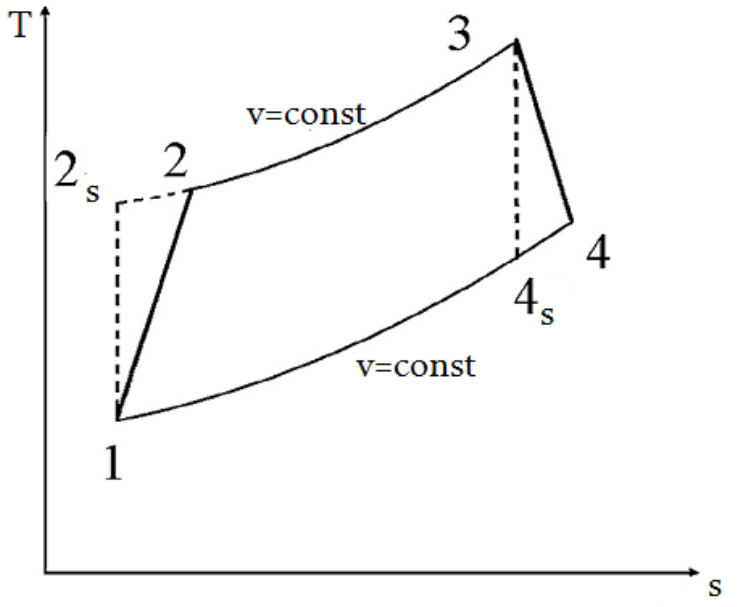

Fig. 3.1 T- s diagram of an air standard Otto cycle model.

Process 1→2 is a reversible adiabatic compression, while process 1→2_s is an irreversible adiabatic process that takes into account the internal irreversibility in the real compression process. The heat addition is an isochoric process 2→3 (v = const). Process 3→4_s is a reversible adiabatic expansion, while 3→4 is an irreversible adiabatic process that takes into account the internal irreversibility in the real expansion process. The heat rejection is an isochoric process 4→1.

3.3. THERMODYNAMIC MODEL ANALYSIS

In most cycle models, the working fluid is assumed to behave as an ideal gas with constant specific heats. But this assumption can be valid only for small temperature differences. For the large temperature-differences encountered in a practical cycle, this assumption cannot be applied. According to Ref. [12], for the temperature range of 200-1000 K, the specific heat with constant pressure can be written as:

$$\left.\begin{array}{c} C_p = 2.506\times10^{-11}T^2 + 1.454\times10^{-7}T^{1.5} - 4.246\times10^{-7}T \\ +3.162\times10^{-5}T^{0.5} + 1.3303 - 1.512\times10^{4}T^{-1.5} + 3.063\times10^{5}T^{-2} \\ -2.212\times10^{7}T^{-3} \end{array}\right\} \ldots\ldots (3.1)$$

Where:

c_p = The constant pressure specific heat (kJ/kg.K).

T = The temperature of gas (K).

According to the relation between constant pressure specific heat and constant volume specific heat:

$$C_p - C_v = Rg \ldots\ldots\ldots\ldots (3.2)$$

Where:

$Rg =$ is the gas constant of the working fluid equal [0.287] (kJ/kg. K).

The constant volume specific heat can be written as follow:

$$\left.\begin{array}{c} c_v = c_p - Rg = 2.506\times10^{-11}T^2 + 1.454\times10^{-7}T^{1.5} - 4.246\times10^{-7}T \\ +3.162\times10^{-5}T^{0.5} + 1.0433 - 1.512\times10^{4}T^{-1.5} + 3.063\times10^{5}T^{-2} \\ -2.212\times10^{7}T^{-3} \end{array}\right\} \ldots (3.3)$$

Where:

c_v = The constant volume specific heat (kJ/kg.K).

Equations (3.1) and (3.3) is based on the assumption that air is an ideal gas mixture containing 78.09% nitrogen, 20.95% oxygen, 0.93% argon, and 0.03% carbon dioxide (on mole basis).

Actually, we find that the specific heat of the elements that compose the air has different degree of dependence on temperature. Some elements specific heats are strongly dependent on temperature, while others are less dependent. Thus, it is more accurate to calculate the specific heat of the mixture as a summation of individual elements specific heats.

The temperature-dependent specific heat at constant pressure for the elements that compose the air takes the general form, (Ferguson C, Kirkpatrick A. 2001).

$$\frac{c_p}{R} = a_1 + a_2T + a_3T^2 + a_4T^3 + a_5T^4 \quad \ldots\ldots\ldots\ldots\ldots\ldots\ldots\ldots\ldots (3.4)$$

Where:

$R =$ the gas constant of the element (kJ/kg K).

$a_1, a_2, \ldots a_5 =$ constants.

The constants in equation (3.4) are given in tables (3.1a) and (3.1b) for the elements that compose the air in addition to the gases that appear as combustion products.

Table 3.1a: Coefficients for species temperature-dependent specific heats [T ≤ 1000K].

i	**Species**	a_1	a_2	a_3	a_4	a_5
1	CO_2	0.24007797E+01	0.87350957E-02	-0.66070875E-05	0.20021861E-08	0.63274039E-15
2	H_2O	0.40701275E+01	-0.11084499E-02	0.41521180E-05	-0.29637404E-08	0.80702103E12
3	N_2	0.36748261E+01	-0.12081500E-02	0.23240102E-05	-0.63217559E-09	-0.22577253E-12
4	O_2	0.36255985E+01	-0.18782184E-02	0.70554544E-05	-0.67635137E-08	0.2155593E-11
5	CO	0.37100928E+01	-0.16190964E-02	0.36923594E-05	-0.20319674E-08	0.23953344E-12
6	H_2	0.30574451E+01	0.26765200E-02	-0.58099162E-05	0.55210391E-08	-0.18122739E-11

Table 4.1b: Coefficients for species temperature-dependent specific heats [1000<T<3200K].

i	**Species**	a_1	a_2	a_3	a_4	a_5
1	CO_2	0.446080E+01	0.309817E-02	-0.123925E-05	0.227413E-09	-0.155259E-13
2	H_2O	0.271676E+01	0.294513E-02	-0.802243E-06	0.102266E-09	-0.484721E-14
3	N_2	0.289631E+01	0.151548E-02	-0.572352E-06	0.998073E-10	-0.652235E-14
4	O_2	0.362195E+01	0.736182E-03	-0.196522E-06	0.362015E10	-0.289456E-14
5	CO	0.298406E+01	0.148913E-02	-0.578996E-06	0.103645E-09	-0.693535E-14
6	H_2	0.310019E+01	0.511194E-03	0.526442E-07	-0.349099E-10	0.369453E-14

In this study we will assume that the air consists of 76.51% nitrogen, 23.44% oxygen, and 0.05% carbon dioxide (on mass basis).

To calculate the values of gas constant for the above gases we must know the values of molecular weight of these gases as shown in Table (3.2).

Table 3.2 Molecular weight of air constituent gases

	Constituent	M (kg/kmol)
1	N_2	28.013
2	O_2	31.999
3	CO_2	44.010

Thus, the specific heat at constant pressure for air can be obtained as follow:

$$C_{p_{air}} = \sum_{i=1}^{n} x_i \, C_{p_i} \quad \ldots\ldots\ldots\ldots\ldots\ldots\ldots\ldots\ldots\ldots\ldots\ldots\ldots\ldots\ldots\ldots\ldots\ldots\ldots\ldots\ldots\ldots\ldots\ldots\ldots\ldots\ldots\ldots 3.5)$$

Where:

C_{p_i} = The specific heat at constant pressure for component ***i*** (kJ/kg.K).

x_i = The mass fraction for component ***i***.

Also, the gas constant for air can be obtained as follow:

$$R_{air} = \sum_{i=1}^{n} \frac{x_i \, R_u}{M_i} \qquad \ldots \quad (3.6)$$

Where:

R_u = The universal gas constant [8.3145] (kJ/kmol.K).

M_i = The molecular weight for component ***i*** (kg/kmol).

Therefore, the specific heat at constant volume for air can be determined as follow:

$$c_{v_{air}} = c_{p_{air}} - R_{air} \qquad \ldots \quad (3.7)$$

But for simplification, we will use the values of specific heat that given in equations (4.2) and (4.3).

After calculating the specific heats values, we can proceed to calculate the rate of heat added and heat rejected as follow:

$$\dot{Q}_{add} = \dot{m} \int_{T_2}^{T_3} C_v \, dT$$

$$= \dot{m} \begin{bmatrix} 8.353 \times 10^{-12} T^3 + 5.816 \times 10^{-8} T^{2.5} - 2.123 \times 10^{-7} T^2 \\ +2.108 \times 10^{-5} T^{1.5} + 1.0433T + 3.024 \times 10^4 T^{-0.5} - 3.063 \times 10^5 T^{-1} \\ +1.106 \times 10^7 T^{-2} \end{bmatrix}_{T_2}^{T_3} \quad (3.8)$$

$$\dot{Q}_{rej} = \dot{m} \int_{T_1}^{T_4} C_v \, dT$$

$$= \dot{m} \begin{bmatrix} 8.353 \times 10^{-12} T^3 + 5.816 \times 10^{-8} T^{2.5} - 2.123 \times 10^{-7} T^2 \\ +2.108 \times 10^{-5} T^{1.5} + 1.0433T + 3.024 \times 10^4 T^{-0.5} - 3.063 \times 10^5 T^{-1} \\ +1.106 \times 10^7 T^{-2} \end{bmatrix}_{T_1}^{T_4} \quad (3.9)$$

Where:

$\dot{m}$ = The mass flow rate of working substance (kg/s).

For adiabatic compression (process 1→2 and adiabatic expansion (process 3→4, the compression and expansion efficiencies can be defined as follow:

$$\eta_c = \frac{T_{2s} - T_1}{T_2 - T_1} \qquad \ldots \quad (3.10)$$

$$\eta_e = \frac{T_3 - T_4}{T_3 - T_{4s}} \qquad \ldots \quad (3.11)$$

These two efficiencies can be used to describe the internal irreversibility of the processes.

Since the values of the specific heats c_p and c_v depends on the temperature, adiabatic exponent $\gamma = c_p/c_v$ will vary with temperature as well. Therefore, the equation often used in reversible adiabatic process or isentropic process with constant γ cannot be used in isentropic process with variable γ. A suitable engineering approximation has been utilized for reversible adiabatic process with variable γ. Any reversible process between *i* and *j* has considered a large numbers of infinitesimally small processes with constant γ. In that case infinitesimally small change in temperature *dT* and volume *dV* of the working fluid takes place which may be represented as follow[14]:

$$TV^{\gamma-1} = (T + dT)(V + dV)^{\gamma-1} \quad \ldots\ldots\ldots\ldots\ldots\ldots\ldots\ldots\ldots\ldots\ldots\ldots\ldots\ldots\ldots\ldots\ldots\ldots\ldots\ldots (3.12)$$

With Newton's binomial of right side of equation (3.12) and betake the small amounts, yields the fallowing relation:

$$(T + dT)(V + dV)^{\gamma-1} = (T + dT)(V^{\gamma-1} + (\gamma - 1)V^{\gamma-2}dV) \quad \ldots\ldots\ldots\ldots\ldots\ldots\ldots (3.13)$$

By rearranging the equation (3.12), we get:

$$(\gamma - 1)\frac{dV}{V} = -\frac{dT}{T} \quad \ldots\ldots\ldots\ldots\ldots\ldots\ldots\ldots\ldots\ldots\ldots\ldots\ldots\ldots\ldots\ldots\ldots\ldots\ldots\ldots\ldots\ldots\ldots\ldots\ldots\ldots (3.14)$$

By dividing the equation (4.7) on $c_{v,air}$ we get:

$$1 = \gamma - \frac{R}{C_v} \quad or \quad (\gamma - 1) = \frac{R}{C_v} \quad \ldots\ldots\ldots\ldots\ldots\ldots\ldots\ldots\ldots\ldots\ldots\ldots\ldots\ldots\ldots\ldots\ldots\ldots\ldots\ldots\ldots\ldots\ldots\ldots\ldots\ldots (3.15)$$

Substituting (γ - 1) into equation (3.14) and rearrange it, yields fallowing relation:

$$R\frac{dV}{V} = -c_v\frac{dT}{T} \quad \ldots\ldots\ldots\ldots\ldots\ldots\ldots\ldots\ldots\ldots\ldots\ldots\ldots\ldots\ldots\ldots\ldots\ldots\ldots\ldots\ldots\ldots\ldots\ldots\ldots\ldots\ldots\ldots\ldots\ldots\ldots\ldots (3.16)$$

By integrating the equation (4 – 16) between *i* and *j* we get:

$$\int_i^j R\frac{dV}{V} = \int_i^j -C_v\frac{dT}{T} \quad \rightarrow \quad R\ln\frac{V_i}{V_j} = c_v\ln\frac{T_j}{T_i} \quad \ldots\ldots\ldots\ldots\ldots\ldots\ldots\ldots\ldots\ldots\ldots\ldots\ldots\ldots\ldots\ldots\ldots\ldots\ldots\ldots\ldots\ldots\ldots\ldots\ldots\ldots\ldots\ldots\ldots\ldots\ldots\ldots (3.17)$$

Where the temperature in equation of c_v is:

$$T = \frac{T_j - T_i}{\ln\frac{T_j}{T_i}} \quad \text{(3.18)}$$

The compression ratio for Otto cycle is defined as follow:

Compression ratio: $$r_v = \frac{V_1}{V_2} \quad \text{(3.19)}$$

We can reformulate the equation (3.17) for reversible compression process ($1 \rightarrow 2_s$) and reversible expansion process ($3 \rightarrow 4_s$) respectively as follow:

$$R \ln r_v = C_v \ln \frac{T_{2s}}{T_1} \quad \text{(3.20)}$$

$$-R \ln(r_v) = C_v \ln \frac{T_{4s}}{T_3} \quad \text{(3.21)}$$

In ideal thermodynamic models there are no heat losses from the system to surrounding, but actually cycle operation there will be certain heat loss from system to the surroundings due to finite temperature differences between working fluid and cylinder wall. The amount of heat loss through the cylinder wall has been assumed to be proportional to the average temperature of heat addition and cylinder wall temperature which is given as follow:

$$\dot{Q}_{loss} = \dot{m}B(T_2 + T_3 - 2T_0) \quad \text{(3.22)}$$

Where:

B = Heat leakage coefficient of the cylinder wall (kJ/kg.K).

T_0 = The average temperature of the working fluid and cylinder walls (K).

Can be obtained T_0 by calculating the logarithmic mean temperature between *T2* and T_3 as follow:

$$T_0 = \frac{T_3 - T_2}{\ln\frac{T_3}{T_2}} \quad \text{(3.23)}$$

There is another type of losses due to piston friction has been considered assuming a dissipation term which represented by friction force which is in linear function of mean piston velocity gives as follow:

$$f_\mu = \mu v$$

$$= \mu \frac{dx}{dt} \quad \text{(3.24)}$$

Where:

μ = Friction coefficient for global losses (N.s/m).

x = Piston displacement (m).

Therefore, the power loss due to friction is given as follow:

$$P_{\mu} = \frac{dW_{\mu}}{dt} = \left(\mu \frac{dx}{dt}.dx\right)/dt = \mu v^2 \quad \ldots\ldots\ldots\ldots\ldots\ldots (3.25)$$

Where:

v = Mean piston speed (m/s).

Mean piston speed can be obtained for four stoke cycle engine as follow:

$$v = 4LN \quad \ldots\ldots\ldots\ldots\ldots\ldots (3.26)$$

Where:

L = Stroke length of the cylinder (m).

N = The rotational speed of the engine (rev/s).

Finally, the net power out and the thermal efficiency can be obtained by the following equations:

$$P_{net} = \dot{Q}_{add} - \dot{Q}_{rej} - P_{\mu} \quad \ldots\ldots\ldots\ldots\ldots\ldots (3.27)$$

$$\eta_{th} = \frac{P_{net}}{\dot{Q}_{add} + \dot{Q}_{loss}} \quad \ldots\ldots\ldots\ldots\ldots\ldots (3.28)$$

3.4. SOLVING METHODOLOGY

Will use MATLAB software to perform the thermodynamic model calculation. For a particular engine, value of initial temperature T_1, maximum temperature T_3, compression ratio r_v, compression efficiency η_c and expansion efficiency η_e are given.

The first assumption for T_{2s} and T_{4s} can be obtained from the following equations by assuming an ideal cycle

$$T_{2s} = T_1 (r_v)^{\gamma - 1} \quad \ldots\ldots\ldots\ldots\ldots\ldots (3.29)$$

$$T_{4s} = T_3 (1/r_v)^{\gamma - 1} \quad \ldots\ldots\ldots\ldots\ldots\ldots (3.30)$$

Assume the value of γ is equal 1.4, substituting the value of T_{2s} in first time and T_{4s} in second time in equation (3.18) to calculate the value of T which will be substituted in the equation of c_v to get it, after that substitute the value of c_v to get the new values of T_{2s} and T_{4s}, these new values are substituted in equations (3.2) and (3.3) to get the new value of c_p and c_v respectively, this procedure will be repeated by iterative scheme until reach to the desired convergence. The values of T_2 and T_4 can be

obtained from equations (3.10) and (3.11). Rate of heat transfer loss and friction loss are obtained from equation (3.22) and equation (3.24) respectively. Finally power output and efficiency of the cycle can be calculated using equation (3.27) and (3.28) respectively.

3.5. PROGRAM FLOW CHART

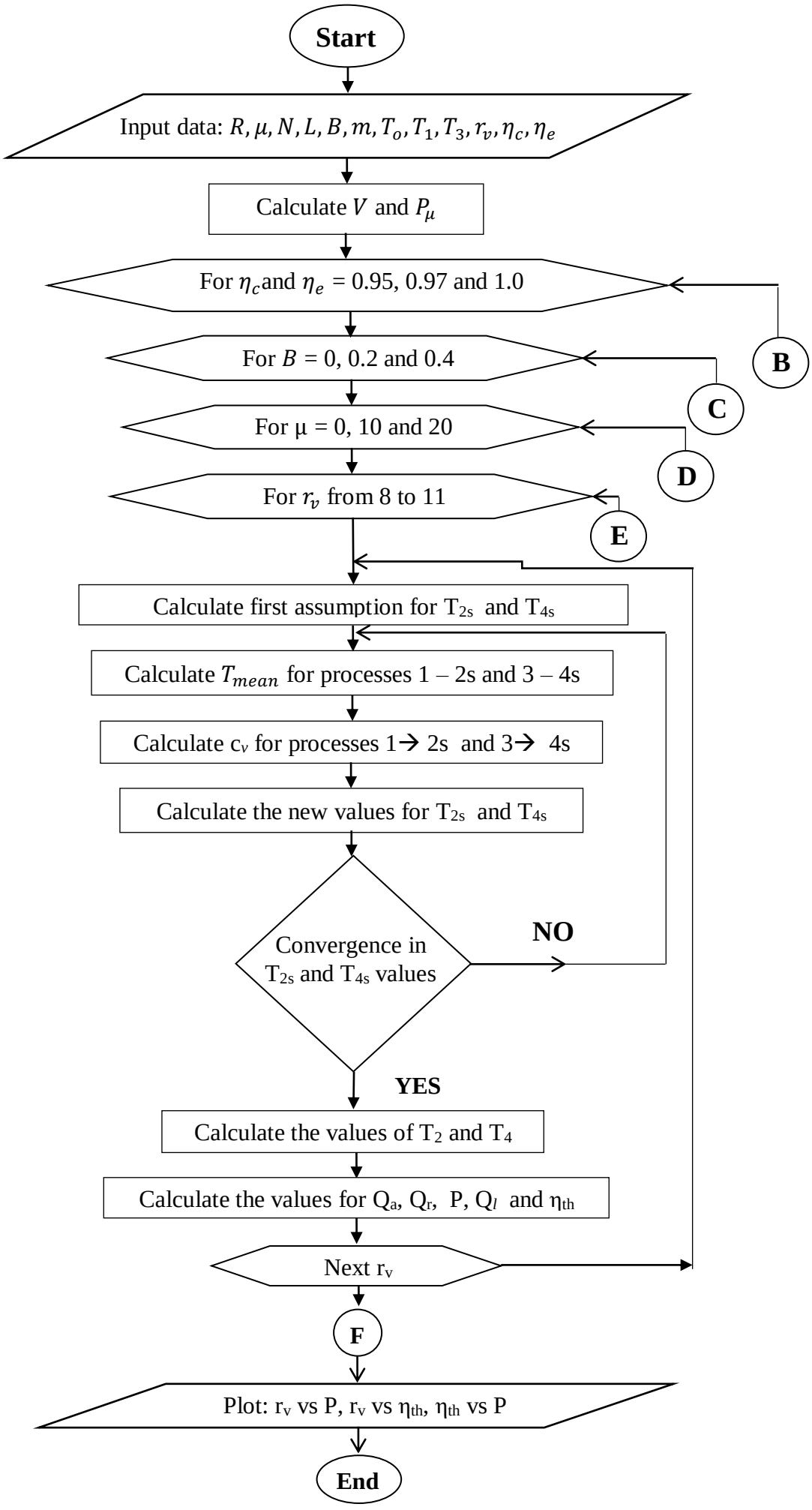
Start
Input data: $R, \mu, N, L, B, m, T_o, T_1, T_3, r_v, \eta_c, \eta_e$
Calculate V and P_μ
For $\eta_c$and η_e = 0.95, 0.97 and 1.0
For B = 0, 0.2 and 0.4
For μ = 0, 10 and 20
For r_v from 8 to 11
B
C
D
E
Calculate first assumption for T_{2s} and T_{4s}
Calculate T_{mean} for processes 1 – 2s and 3 – 4s
Calculate c_v for processes 1→ 2s and 3→ 4s
Calculate the new values for T_{2s} and T_{4s}
Convergence in T_{2s} and T_{4s} values
NO
YES
Calculate the values of T_2 and T_4
Calculate the values for Q_a, Q_r, P, Q_l and η_{th}
Next r_v
F
Plot: r_v vs P, r_v vs η_{th}, η_{th} vs P
End

CHAPTER IV

RESUITS AND DISCUSSION

CHAPTER IV
RESUITS AND DISCUSSION

4.1. INTRODUCTION

In this chapter the results that obtained from the program for various parameters variability, such as effect of non-linear variable specific heats, effect of internal irreversibility, effect of heat losses and effect of friction losses are illustrated discussed and compared with similar results that obtained in previous studies.

4.2. THERMODYNAMIC MODEL INPUT DATA DETAILES

For this model will assume the technical and thermodynamic engine specifications shown in table 4.1

Table 4.1: The technical and thermodynamic engine specifications

Engine Type	4 Stroke Otto Engine
No. of cylinders ($\boldsymbol{n}$)	4 cylinders
Bore ($\boldsymbol{D}$)	91.1 mm
Stroke ($\boldsymbol{L}$)	77.5 mm
Volumetric efficiency ($\boldsymbol{\eta_v}$)	95%
Rotational speed ($\boldsymbol{N}$)	1800 rev/min
Inlet air temperature ($\boldsymbol{T_1}$)	300 K
Peak temperature ($\boldsymbol{T_3}$)	2500 K
Inlet air density ($\boldsymbol{\rho_a}$)	1.2 kg/m^3
Compression ratio ($\boldsymbol{r_v}$)	Vary from 2 to 10.5 with increment 1
Heat leakage coefficient ($\boldsymbol{B}$)	Vary from 0 kJ/kg.K to 0.4 kJ/kg.K with increment 0.2
Friction coefficient for global losses ($\boldsymbol{\mu}$)	Vary from 0 N.s/m to 50 N.s/m with increment 100
Compression efficiency ($\boldsymbol{\eta_c}$)	Three values: 0.95, 0.97 and 1.00
Expansion efficiency ($\boldsymbol{\eta_e}$)	Three values: 0.95, 0.97 and 1.00
Gas constant for air ($\boldsymbol{R}$)	0.287 kJ/kg.K

Depending on the data above, will perform model calculations and presenting results according to the effect of each parameters mentioned above as shown in the following points.

4.3. EFFECT OF INTERNAL IRREVERSIBILITY

In this section we will discuss the effect of internal irreversibility of the engine performance parameters at fixed cut-off ratio and fixed ambient temperature, also without the presence of friction loss and heat loss,

Show in Fig. 4.1 the relation between the compression ratio (r_v) and net output power (P) for 3 different values of compression and expansion efficiencies.

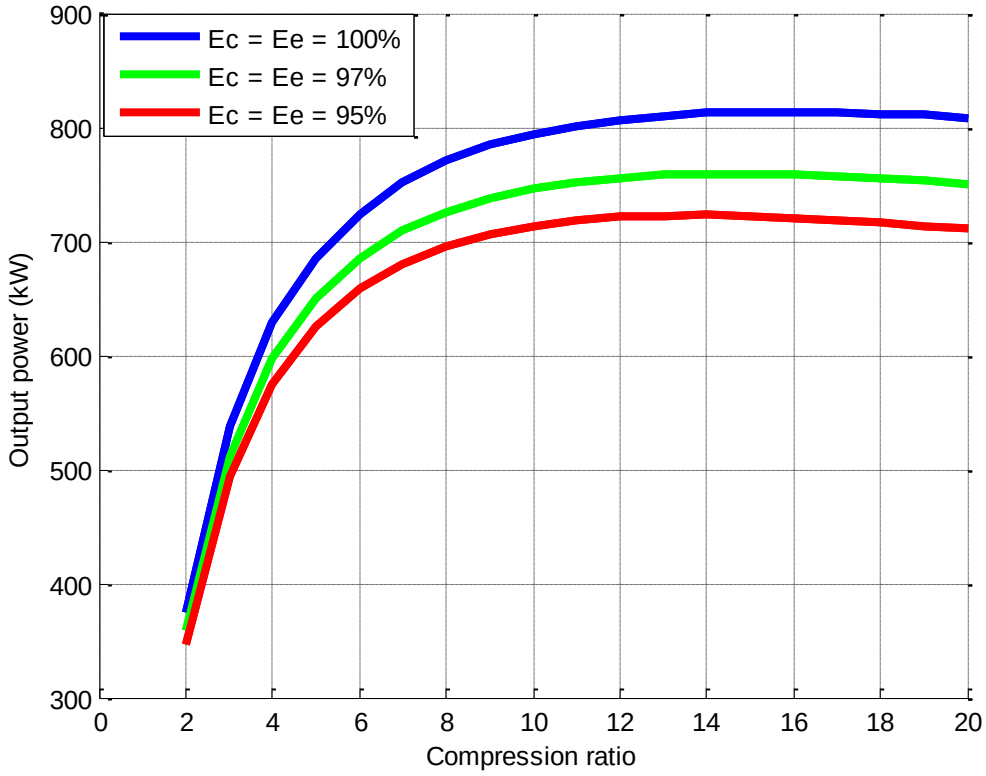

Fig. 4.1 Effect of internal irreversibility on output power (P)

From Fig. 4.1 it's clear that when both of compression and expansion efficiencies increase, the output power values corresponding to higher efficiencies becomes greater than that values corresponding to lower efficiencies for all values of compression ratio.

The output power corresponding to the compression values approximately from 1 to 15 increases rapidly for all values of both of compression and expansion efficiencies, after that the output power corresponding to the remaining values of compression ratio decreasing sharply for all values of both of compression and expansion efficiencies.

Show in Fig. 4.2 the relation between the compression ratio (r_v) and thermal efficiency (η_{th}) for 3 different values of compression and expansion efficiencies.

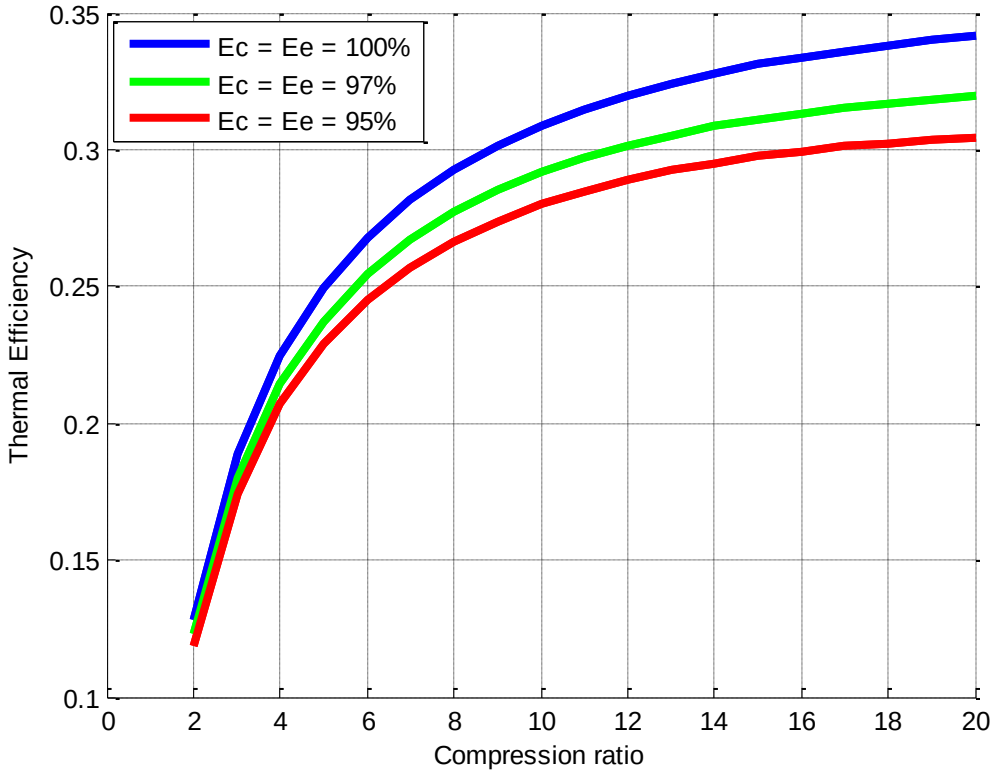

Fig. 4.2 Effect of internal irreversibility on thermal efficiency (η_{th})

From Fig. 4.2 it's clear that the effect of both of compression and expansion efficiencies on thermal efficiency it similar to that effect on output power, but for the thermal efficiency values corresponding to the compression values above 20 approximately decreasing slightly.

Show in Fig. 5.3 the relation between thermal efficiency (η_{th}) and net output power (P) for 3 different values of compression and expansion efficiencies.

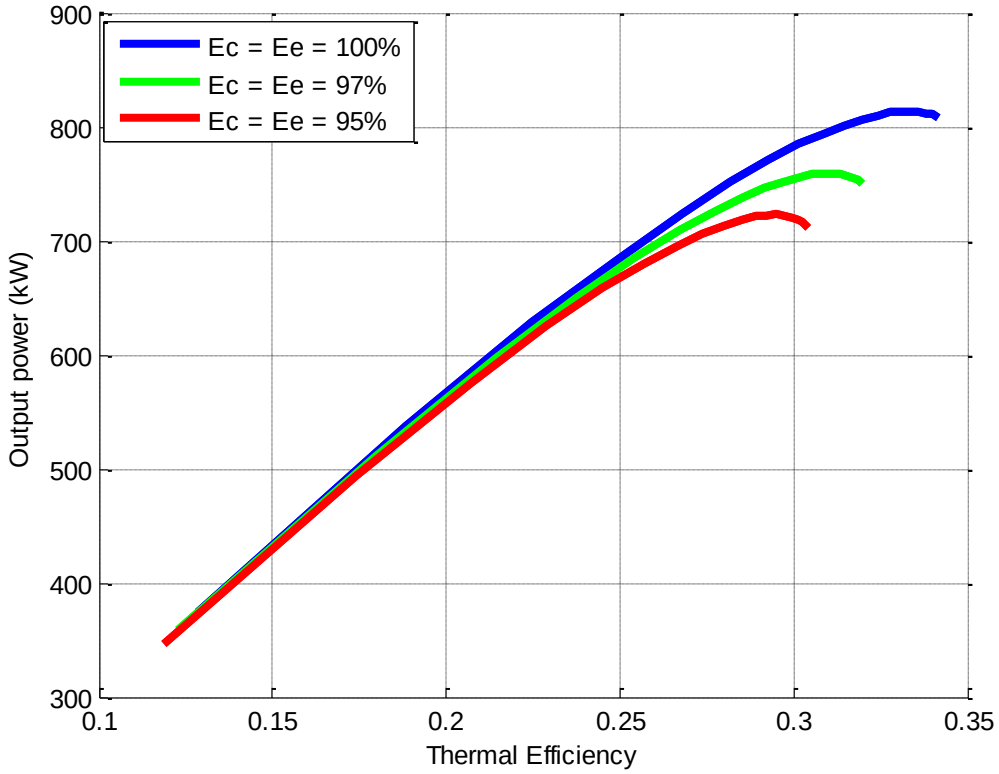

Fig. 5.3 Thermal efficiency (η_{th}) versus output power (P) with respect of internal irreversibility effect

From Fig. 4.3 it's clear that the effect of both of compression and expansion efficiencies on net output power versus thermal efficiency characteristic is decreasing both of them when they both of efficiencies is decrease, also at a specific point on any curve we found peak output power is not identical with maximum thermal efficiency; but we found the value of thermal efficiency corresponding to peak output power less than maximum power.

5.4. EFFECT OF HEAT LOSS

In this section we will discuss the effect of heat loss on the engine performance parameters also at fixed cut-off ratio and fixed ambient temperature, but without the presence of friction loss, and assumed reversible compression and expansion processes (i.e. compression and expansion efficiencies are equal 100%). Heat loss is effect only on the amount of heat addition, thus the heat loss effect in the thermal efficiency.

Show in Fig. 4.4 the relation between the compression ratio (r_v) and thermal efficiency (η_{th}) for 3 different values of heat leakage coefficient.

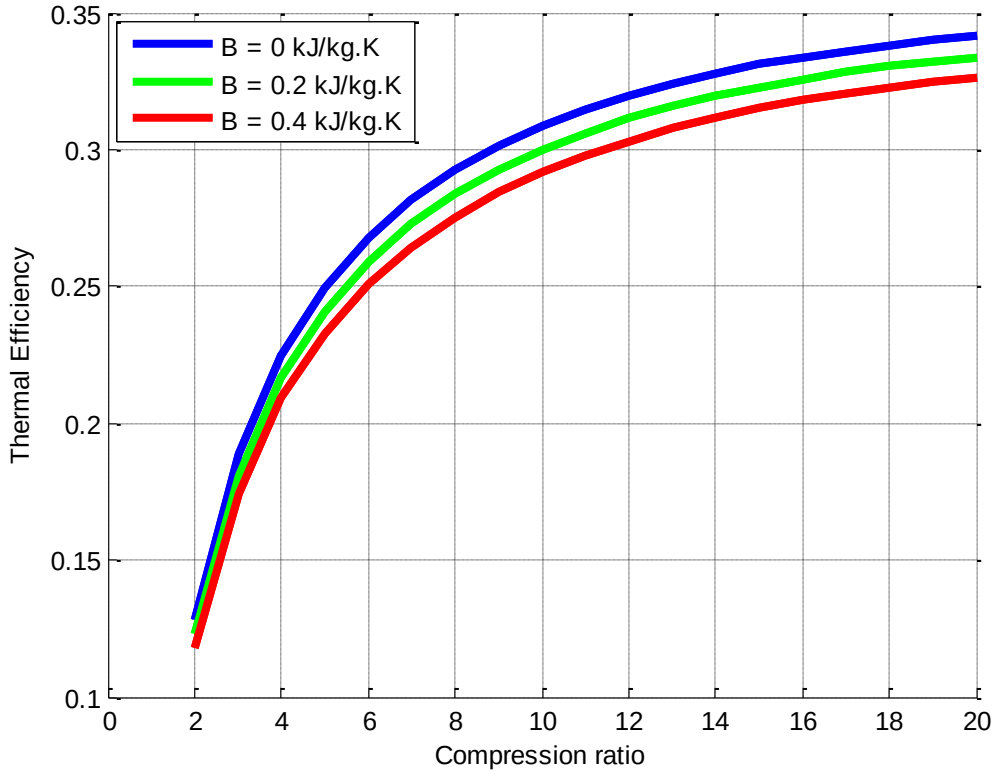

Fig. 4.4 Effect of heat loss on thermal efficiency (η_{th})

From Fig. 4.4 it's clear that when the coefficient of heat leakage decreases, the amount of heat addition values corresponding to lower heat leakage coefficient becomes greater than that values corresponding to higher heat leakage coefficient for all values of compression ratio, with taking into account that the values of output power are not change. Thus the effect of heat leakage coefficient on the thermal efficiency it will be similar to that effect on the amount of heat addition.

The thermal efficiency corresponding to the compression values approximately increases rapidly for all values of heat leakage coefficient.

Also in specific value of compression ratio, the difference between the value of thermal efficiency corresponding to heat leakage coefficient and the value of thermal efficiency corresponding to another heat leakage coefficient is a significant difference.

Show in Fig. 4.5 the relation between thermal efficiency (η_{th}) and net output power (P)for 3 different values of heat leakage coefficient.

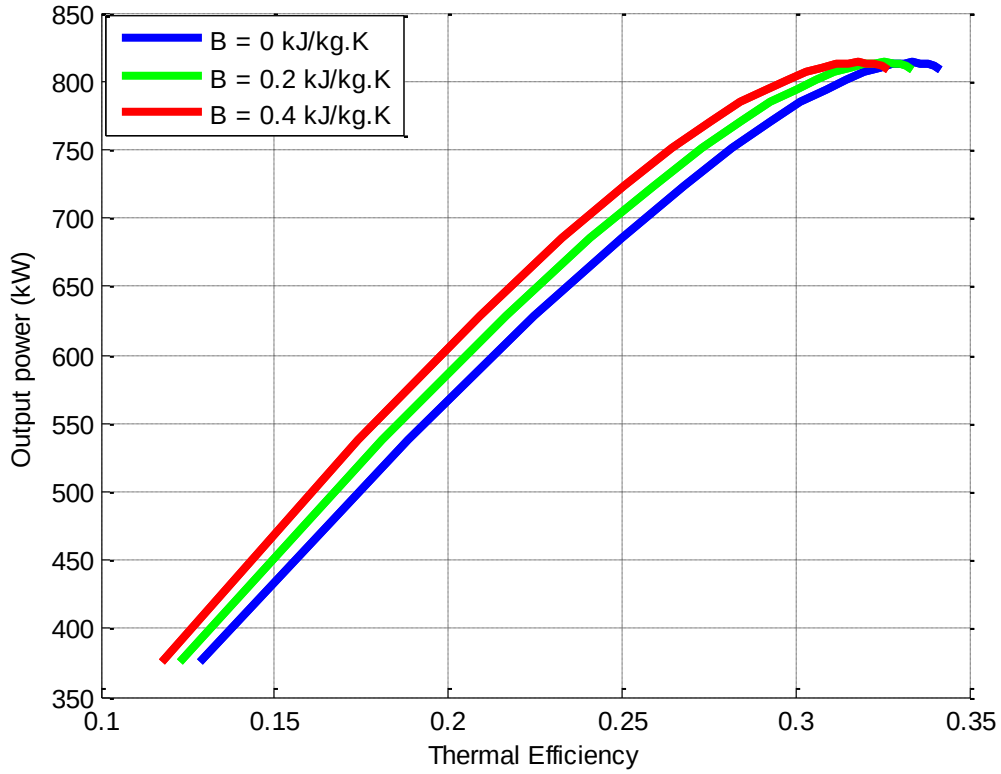

Fig. 5.5: Thermal efficiency (η_{th}) versus output power (P) with respect of heat loss effect

From Fig. 4.3 it's clear that the effect of heat leakage coefficient on net output power versus thermal efficiency characteristic is decreasing the thermal efficiency only when the heat leakage coefficient is increase, because the heat leakage coefficient effect just on the amount of heat addition and has no effect on the output power.

4.5. EFFECT OF FRICTION LOSS

In this section we will discuss the effect of friction loss on the engine performance parameters also at fixed cut-off ratio and fixed ambient temperature, but without the presence of heat loss, and assumed reversible compression and expansion processes (i.e. compression and expansion efficiencies are equal 100%). Friction loss actually effect on the net output power and heat transfer from or to engine. But can be assume that it affects only on the net output power because it effect on the amount of heat transfer is very small and can be neglected.

Show in Fig. 4.6 the relation between the compression ratio (r_v) and net output power (P) for 3 different values of friction coefficients.

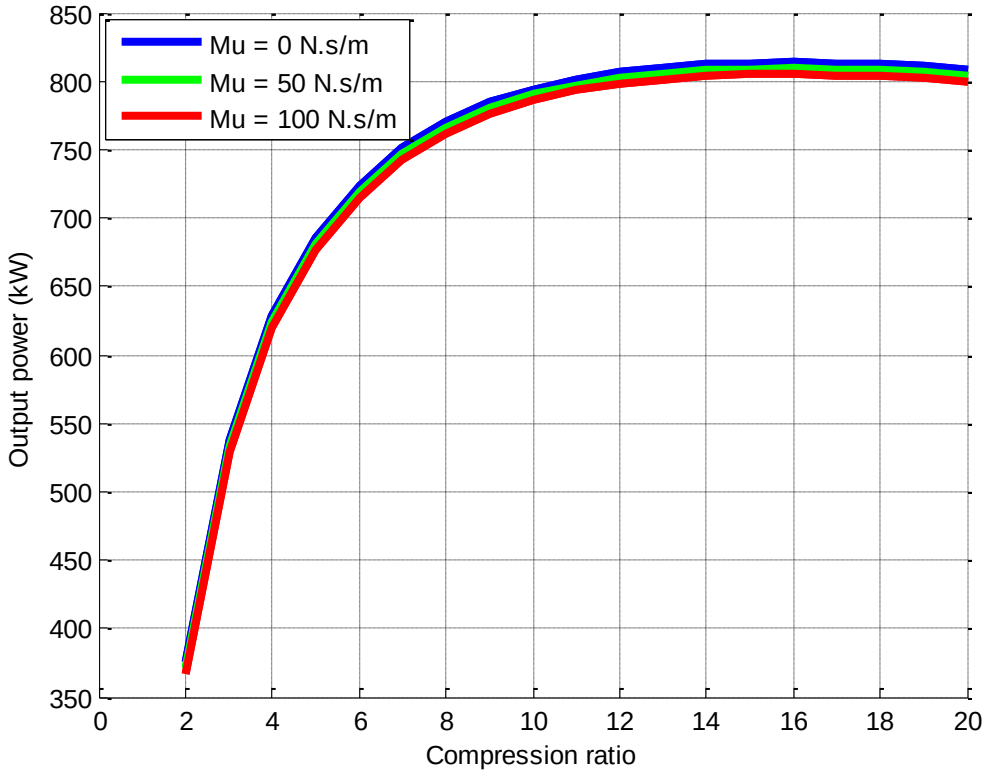

Fig. 4.6: Effect of friction loss on output power (P)

From Fig. 4.6 it's clear that when the coefficient of friction increases, the output power decrease, but the amount of decreasing in the output power is not large.

The output power corresponding to the compression values approximately from 1 to 17 increases rapidly for all values of friction coefficients, after that the output power corresponding to the remaining values of compression ratio decreasing sharply for all values of friction coefficients.

Show in Fig. 4.7 the relation between the compression ratio (r_v) and thermal efficiency (η_{th}) for 3 different values of friction coefficient.

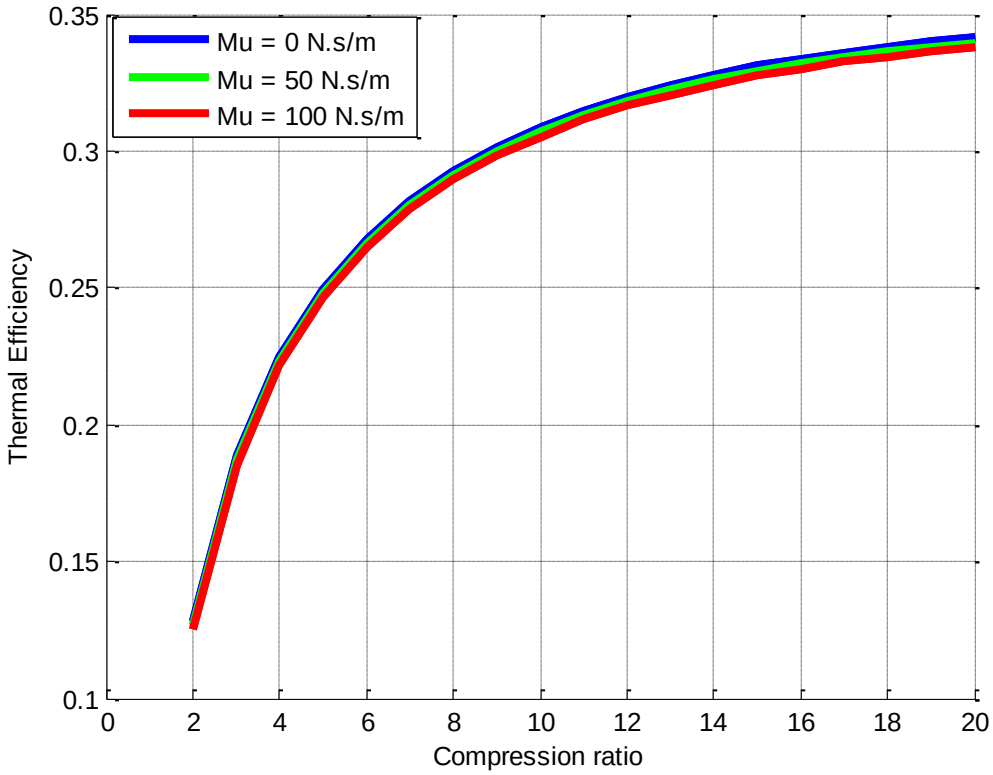

Fig. 5.7: Effect of friction loss on thermal efficiency (η_{th})

From Fig. 4.7 it's clear that when the coefficient of friction increases, the output power values decrease for all values of compression ratio as mentioned previously, with taking into account that the amounts of heat addition are not change. Thus the effect of friction coefficient on the thermal efficiency it will be similar to that effect on the output power.

The thermal efficiency corresponding to the compression values approximately increases rapidly for all values of friction coefficient.

Also in specific value of compression ratio, the difference between the value of thermal efficiency corresponding to friction coefficient and the value of thermal efficiency corresponding to another friction coefficient is a relatively small difference.

Show in Fig. 5.8 the relation between thermal efficiency (η_{th}) and net output power (P) for 3 different values of friction coefficient.

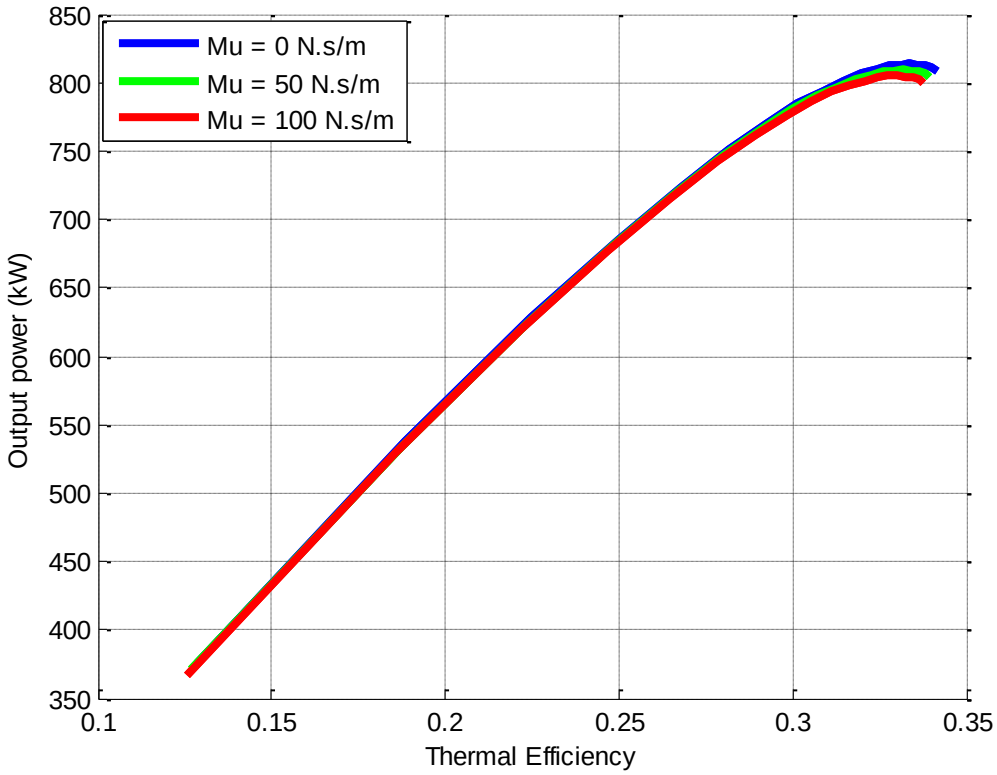

Fig. 5.8: Thermal efficiency (η_{th}) versus output power (P)
with respect of friction loss effect

From fig. 4.8 it's clear that the effect of friction coefficient on net output power versus thermal efficiency characteristic is decreasing both of them when the friction coefficient is increase.

The effect of friction coefficient variation is quite similar to that effect caused by the both of compression and expansion efficiency as mentioned previously.

CHAPTER V

CONCLUSIONS AND RECOMMENDATIONS

CHAPTER V

CONCLUSIONS AND RECOMMENDATIONS

5.1. CONCLUSIONS

In chapters three and four, the calculations were performed on the Otto cycle thermodynamic model and the results that obtained from the model were shown. The results show that the following conclusions:

1. The differences in results obtained from the thermodynamic model compared with the results obtained from experiments are not too considerable.
2. The both of compression and expansion efficiencies do not cause a considerable influence on the output power and the thermal efficiency.
3. Heat loss has a significant effect on the thermal efficiency, where the difference between the highest thermal efficiency corresponding to the heat leakage coefficient 0.4 kJ/kg.K and the highest thermal efficiency without heat loss (i.e. heat leakage coefficient equal zero) is about 12% and this is significant value.
4. Friction loss has no considerable effect on the output power and the thermal efficiency such as the effect of both of compression and expansion efficiencies.
5. Can benefit from these results that have been obtained from this thermodynamic model in the design of the engine.

5.2. RECOMMENDATIONS

According to the conclusions that mentioned previously, we will recommend the following:

1. Applying these thermodynamic model assumptions into programs that simulate the engine work and comparing the results obtained from the simulation with the results that obtained from this model.
2. The specific heats equations, which depending on the temperature variation must be more precise in order to be a thermodynamic model as close as possible to reality.
3. The losses that occur in the engine must be determined accurately so as to get more accurate results.

References

Abu-Nada, Thermodynamic Modeling of Spark-Ignition Engine: Effect of Temperature Dependent Specific Heats, Int. Comm. Heat Mass Transfer, 32(8), pp. 1045-1056, (2007),

Angulo-Brown F., J Fernandez-Betanzos and C A Diaz-Pico(1994). Compression Ratio of an Optimized Air Standard Otto-Cycle Model. Eur. J. Phys., 15 (1994) 38-42.

Angulo-Browny J. A., Rocha-Mart´ınezz and Navarrete-Gonz´alez T. D. (1996), A non-Endoreversible Otto Cycle Model: Improving Power output And Efficiency, J. Phys. D: Appl. Phys., 29 (1996) 80-83.

Bjarne Andresen, Finite-Time Thermodynamics and Thermodynamic Length. Rev Ge'n Therm (1996) 35, 647-650.

Chen. L., Performance of A Reciprocating Endoreversible Brayton Cycle With Variable Specific Heats of Working Fluid. Termotehnica. 1 (3), pp. 19-23. (2008).

Curzon F. L. and Ahlborn B., Efficiency of a Carnot Engine at Maximum Power Output. American Journal of Physics. 43 (22), pp. 22-24, (1975).

Ferguson C, Kirkpatrick A. (2001). Internal Combustion Engines: Applied Thermosciences. Wiley: New York.

Kieu T.D., Eur. Phys. J. D 39, 115 (2006)

Kieu T.D., Phys. Rev. Lett. 93, 140403 (2004)

Setiadipura T., Suwoto, Zuhair, Bakhri S., G.R. Sunaryo, Power Peaking Effect of Otto Fuel Scheme Pebble Bed Reactor. Journal of Physics: Conf. Series 962 (2018) 012065.

Yanlin Ge a, Lingen Chen, Fengrui Sun, Chih Wub, Thermodynamic Simulation of Performance of an Otto Cycle With Heat Transfer and Variable Specific Heats of Working Fluid. International Journal of Thermal Sciences 44 (2005) 506–511.

Yanlin Ge, Lingen Chen , Xiaoyong Qin, Effect of specific heat variations on irreversible Otto cycle performance. journal homepage (2008): www.elsevier.com/locate/ijhmt

Yanlin GE, Lingen Chen and Fengrui Sun (2010). Finite Time Thermodynamic Modeling And Analysis For An Irreversible Atkinson Cycle. Journal of Thermal Science. 14 (4), pp. 887-896

Yanlin Ge, Lingen Chen and Fengrui Sun, The Effects Of Variable Specific Heats of Working Fluid on the Performance of an Irreversible Otto cycle. Postgraduate School, Naval University of Engineering,Wuhan 430033, P.R. China, (2005).

Yanlin Ge, Lingen Chen, Fengrui Sun, Finite-Time Thermodynamic Modelling and Analysis of an Irreversible Otto-cycle. Postgraduate School, Naval University of Engineering, Wuhan, 430033, PR China, (2008).

Yunus A. Cengel, Michael A. Boles, Thermodynamics an engineering approach. 8th ed. London: McGraw-Hill. (2015).

APPENDIX

Appendix A
Program code

Otto cycle program

```
clc
cp=xlsread('result.xls',1,'A1:H1');
cv=xlsread('result.xls',1,'A2:H2');
qa=xlsread('result.xls',1,'A3:H3');
qr=xlsread('result.xls',1,'A4:H4');
R=0.287; %Gas constant for air (kJ/kg.K)
Mu=[0 50 100]; %Friction coefficient for global losses (N.s/m)
N=1800; %Rotational speed (rev/min)
L=0.0775; %Stroke (m)
V=4*L*N/60; %Piston speed (m/s)
Pu=Mu.*V^2/1000; %Power loss due to friction (kW)
B=[0 0.2 0.4]; %Heat leakage coefficient (kJ/kg.K)
ma=1; % Air mass flow rate (kg/s)
m=0.07572; %Fuel mass flow rate (kg/s)
m=ma+mf; %Mixture mass flow rate (kg/s)
T1=300; %Inlet temperature (K)
T3=2500; %Maximum temperature (K)
rv=1:200; %Compression ratio
T2sn(1)=1;
T4sn(1)=1;
EE=1;
E=[1 0.97 0.95]; %Isentropic efficiency for compression and expansion
%-------------------------------------------------------------------
%----------------- Effect of isentropic efficiency -----------------
%-------------------------------------------------------------------
for u=1:length(B)
    for k=1:length(E)
        for j=1:length(rv)
            T2si(j)=T1*(rv(j)^0.4);
            T4si(j)=T3*((1/rv(j))^0.4);
            T2s(j)=T2si(j);
            T4s(j)=T4si(j);
            for h=1:500
                Tmean12(j)=(T2s(j)-T1)/log(T2s(j)/T1);
                Tmean34(j)=(T4s(j)-T3)/log(T4s(j)/T3);
                Cv1(j)=cv(1)*(Tmean12(j)^2)+cv(2)*(Tmean12(j)^1.5)-
cv(3)*(Tmean12(j))+cv(4)*(Tmean12(j)^0.5)+cv(5)-cv(6)*(Tmean12(j)^-
1.5)+cv(7)*(Tmean12(j)^-2)-cv(8)*(Tmean12(j)^-3);
                Cv2(j)=cv(1)*(Tmean34(j)^2)+cv(2)*(Tmean34(j)^1.5)-
cv(3)*(Tmean34(j))+cv(4)*(Tmean34(j)^0.5)+cv(5)-cv(6)*(Tmean34(j)^-
1.5)+cv(7)*(Tmean34(j)^-2)-cv(8)*(Tmean34(j)^-3);
                T2s(j)=T1*exp((R/Cv1(j))*log(rv(j)));
                T4s(j)=T3*exp(-(R/Cv2(j))*log(rv(j)));
            end
            T2(j)=((T2s(j)-T1)/E(k))+T1;
            T4(j)=T3-(E(k)*(T3-T4s(j)));
            Qa(j)=m*((qa(1)*(T3-T2(j))^3)+(qa(2)*(T3-T2(j))^2.5)-
(qa(3)*(T3-T2(j))^2)+(qa(4)*(T3-T2(j))^1.5)+(qa(5)*(T3-
T2(j)))+(qa(6)*(T3-T2(j))^-0.5)-(qa(7)*(T3-T2(j))^-1)+(qa(8)*(T3-
T2(j))^-2));
            Qr(j)=m*((qr(1)*(T4(j)-T1)^3)+(qr(2)*(T4(j)-T1)^2.5)-
(qr(3)*(T4(j)-T1)^2)+(qr(4)*(T4(j)-T1)^1.5)+(qr(5)*(T4(j)-
```

```
T1))+(qr(6)*(T4(j)-T1)^-0.5)-(qr(7)*(T4(j)-T1)^-1)+(qr(8)*(T4(j)-T1)^-
2));
            P(j)=Qa(j)-Qr(j);
            T0(j)=(T3-T2(j))/(log(T3/T2(j)));
            Ql(j)=m*B(1)*(T2(j)+T3-2*T0(j));
            Eth(j)=P(j)/(Qa(j)+Ql(j));
            Data_E(EE,j)=P(j);
            Data_E(EE+1,j)=Eth(j);
        end
        EE=EE+2;
    end

end
figure(1)
hold on
plot(rv,Data_E(1,:),'b-','LineWidth',3)
plot(rv,Data_E(3,:),'g-','LineWidth',3)
plot(rv,Data_E(5,:),'r-','LineWidth',3)
xlabel('Compression ratio')
ylabel('Output power (kW)')
legend('Ec = Ee = 100%','Ec = Ee = 97%','Ec = Ee = 95%')
%axis ([0 200 0 5])
grid on
figure(2)
hold on
plot(rv,Data_E(2,:),'b-','LineWidth',3)
plot(rv,Data_E(4,:),'g-','LineWidth',3)
plot(rv,Data_E(6,:),'r-','LineWidth',3)
xlabel('Compression ratio')
ylabel('Thermal Efficiency')
legend('Ec = Ee = 100%','Ec = Ee = 97%','Ec = Ee = 95%')
%axis ([0 200 0 0.4])
grid on
figure(3)
hold on
plot(Data_E(2,:),Data_E(1,:),'b-','LineWidth',3)
plot(Data_E(4,:),Data_E(3,:),'g-','LineWidth',3)
plot(Data_E(6,:),Data_E(5,:),'r-','LineWidth',3)
xlabel('Thermal Efficiency')
ylabel('Output power (kW)')
legend('Ec = Ee = 100%','Ec = Ee = 97%','Ec = Ee = 95%')
%axis ([0 0.4 0 5])
grid on
%-------------------------------------------------------------------
%---------------------- Effect of heat losses ----------------------
%-------------------------------------------------------------------
QL=1;
for u=1:length(B)
        for k=1:length(E)
            for j=1:length(rv)
                T2si(j)=T1*(rv(j)^0.4);
                T4si(j)=T3*((1/rv(j))^0.4);
                T2s(j)=T2si(j);
                T4s(j)=T4si(j);
                for h=1:500
                    Tmean12(j)=(T2s(j)-T1)/log(T2s(j)/T1);
                    Tmean34(j)=(T4s(j)-T3)/log(T4s(j)/T3);

Cv1(j)=cv(1)*(Tmean12(j)^2)+cv(2)*(Tmean12(j)^1.5)-
cv(3)*(Tmean12(j))+cv(4)*(Tmean12(j)^0.5)+cv(5)-cv(6)*(Tmean12(j)^-
1.5)+cv(7)*(Tmean12(j)^-2)-cv(8)*(Tmean12(j)^-3);
```

```
Cv2(j)=cv(1)*(Tmean34(j)^2)+cv(2)*(Tmean34(j)^1.5)-
cv(3)*(Tmean34(j))+cv(4)*(Tmean34(j)^0.5)+cv(5)-cv(6)*(Tmean34(j)^-
1.5)+cv(7)*(Tmean34(j)^-2)-cv(8)*(Tmean34(j)^-3);
                    T2s(j)=T1*exp((R/Cv1(j))*log(rv(j)));
                    T4s(j)=T3*exp(-(R/Cv2(j))*log(rv(j)));
                end
                T2(j)=((T2s(j)-T1)/E(1))+T1;
                T4(j)=T3-(E(1)*(T3-T4s(j)));
                Qa(j)=m*((qa(1)*(T3-T2(j))^3)+(qa(2)*(T3-T2(j))^2.5)-
(qa(3)*(T3-T2(j))^2)+(qa(4)*(T3-T2(j))^1.5)+(qa(5)*(T3-
T2(j)))+(qa(6)*(T3-T2(j))^-0.5)-(qa(7)*(T3-T2(j))^-1)+(qa(8)*(T3-
T2(j))^-2));
                Qr(j)=m*((qr(1)*(T4(j)-T1)^3)+(qr(2)*(T4(j)-T1)^2.5)-
(qr(3)*(T4(j)-T1)^2)+(qr(4)*(T4(j)-T1)^1.5)+(qr(5)*(T4(j)-
T1))+(qr(6)*(T4(j)-T1)^-0.5)-(qr(7)*(T4(j)-T1)^-1)+(qr(8)*(T4(j)-T1)^-
2));
                P(j)=Qa(j)-Qr(j);
                T0(j)=(T3-T2(j))/(log(T3/T2(j)));
                Ql(j)=m*B(u)*(T2(j)+T3-2*T0(j));
                Eth(j)=P(j)/(Qa(j)+Ql(j));
                Data_ql(QL,j)=P(j);
                Data_ql(QL+1,j)=Eth(j);
            end
        end
    QL=QL+2;
end
figure(4)
hold on
plot(rv,Data_ql(2,:),'b-','LineWidth',3)
plot(rv,Data_ql(4,:),'g-','LineWidth',3)
plot(rv,Data_ql(6,:),'r-','LineWidth',3)
xlabel('Compression ratio')
ylabel('Thermal Efficiency')
legend('B = 0 kJ/kg.K','B = 0.2 kJ/kg.K','B = 0.4 kJ/kg.K')
grid on
figure(5)
hold on
plot(Data_ql(2,:),Data_ql(1,:),'b-','LineWidth',3)
plot(Data_ql(4,:),Data_ql(3,:),'g-','LineWidth',3)
plot(Data_ql(6,:),Data_ql(5,:),'r-','LineWidth',3)
xlabel('Thermal Efficiency')
ylabel('Output power (kW)')
legend('B = 0 kJ/kg.K','B = 0.2 kJ/kg.K','B = 0.4 kJ/kg.K')
grid on
%-----------------------------------------------------------------------
%--------------------- Effect of friction power ---------------------
%-----------------------------------------------------------------------
PU=1;
for u=1:length(Mu)
        for k=1:length(E)
            for j=1:length(rv)
                T2si(j)=T1*(rv(j)^0.4);
                T4si(j)=T3*((1/rv(j))^0.4);
                T2s(j)=T2si(j);
                T4s(j)=T4si(j);
                for h=1:500
                    Tmean12(j)=(T2s(j)-T1)/log(T2s(j)/T1);
                    Tmean34(j)=(T4s(j)-T3)/log(T4s(j)/T3);

Cv1(j)=cv(1)*(Tmean12(j)^2)+cv(2)*(Tmean12(j)^1.5)-
```

```
cv(3)*(Tmean12(j))+cv(4)*(Tmean12(j)^0.5)+cv(5)-cv(6)*(Tmean12(j)^-
1.5)+cv(7)*(Tmean12(j)^-2)-cv(8)*(Tmean12(j)^-3);

Cv2(j)=cv(1)*(Tmean34(j)^2)+cv(2)*(Tmean34(j)^1.5)-
cv(3)*(Tmean34(j))+cv(4)*(Tmean34(j)^0.5)+cv(5)-cv(6)*(Tmean34(j)^-
1.5)+cv(7)*(Tmean34(j)^-2)-cv(8)*(Tmean34(j)^-3);
                    T2s(j)=T1*exp((R/Cv1(j))*log(rv(j)));
                    T4s(j)=T3*exp(-(R/Cv2(j))*log(rv(j)));
                end
                T2(j)=((T2s(j)-T1)/E(1))+T1;
                T4(j)=T3-(E(1)*(T3-T4s(j)));
                Qa(j)=m*((qa(1)*(T3-T2(j))^3)+(qa(2)*(T3-T2(j))^2.5)-
(qa(3)*(T3-T2(j))^2)+(qa(4)*(T3-T2(j))^1.5)+(qa(5)*(T3-
T2(j)))+(qa(6)*(T3-T2(j))^-0.5)-(qa(7)*(T3-T2(j))^-1)+(qa(8)*(T3-
T2(j))^-2));
                Qr(j)=m*((qr(1)*(T4(j)-T1)^3)+(qr(2)*(T4(j)-T1)^2.5)-
(qr(3)*(T4(j)-T1)^2)+(qr(4)*(T4(j)-T1)^1.5)+(qr(5)*(T4(j)-
T1))+(qr(6)*(T4(j)-T1)^-0.5)-(qr(7)*(T4(j)-T1)^-1)+(qr(8)*(T4(j)-T1)^-
2));
                Pu(u)=Mu(u)*V^2/1000;
                P(j)=Qa(j)-Qr(j)-Pu(u);
                Eth(j)=P(j)/Qa(j);
                Data_pu(PU,j)=P(j);
                Data_pu(PU+1,j)=Eth(j);
            end
        end
    PU=PU+2;
end
figure(6)
hold on
plot(rv,Data_pu(1,:),'b-','LineWidth',3)
plot(rv,Data_pu(3,:),'g-','LineWidth',3)
plot(rv,Data_pu(5,:),'r-','LineWidth',3)
xlabel('Compression ratio')
ylabel('Output power (kW)')
legend('Mu = 0 N.s/m','Mu = 50 N.s/m','Mu = 100 N.s/m')
%axis ([0 200 0 5])
grid on
figure(7)
hold on
plot(rv,Data_pu(2,:),'b-','LineWidth',3)
plot(rv,Data_pu(4,:),'g-','LineWidth',3)
plot(rv,Data_pu(6,:),'r-','LineWidth',3)
xlabel('Compression ratio')
ylabel('Thermal Efficiency')
legend('Mu = 0 N.s/m','Mu = 50 N.s/m','Mu = 100 N.s/m')
%axis ([0 50 0 0.4])
grid on
figure(8)
hold on
plot(Data_pu(2,:),Data_pu(1,:),'b-','LineWidth',3)
plot(Data_pu(4,:),Data_pu(3,:),'g-','LineWidth',3)
plot(Data_pu(6,:),Data_pu(5,:),'r-','LineWidth',3)
xlabel('Thermal Efficiency')
ylabel('Output power (kW)')
legend('Mu = 0 N.s/m','Mu = 50 N.s/m','Mu = 100 N.s/m')
%axis ([0 0.4 0 5])
grid on
```